NASA TECHNICAL MEMORANDUM

NASA TM X-52948

NASA TM X-52948

A PARAMETRIC THERMAL ANALYSIS OF AN ISOTOPE BRAYTON HEAT SOURCE DESIGN DURING STEADY STATE OPERATION

by Raymond K. Burns
Lewis Research Center
Cleveland, Ohio
December, 1970

This information is being published in preliminary form in order to expedite its early release.

A PARAMETRIC THERMAL ANALYSIS OF AN ISOTOPE BRAYTON HEAT SOURCE DESIGN DURING STEADY STATE OPERATION

by Raymond K. Burns

Lewis Research Center

Cleveland, Ohio

NATIONAL AERONAUTICS AND SPACE ADMINISTRATION

ABSTRACT

Results of a thermal analysis to predict the internal temperatures in an isotope heat source (a design based on Pioneer technology) during Brayton power system operation are presented. A range of heat source and heat source heat exchanger emissivities which could be expected, a range of heat source fuel load around the nominal 400-watt value, and a range of heat exchanger temperatures around the nominal value for a 1600° F turbine inlet temperature were considered. The type of heat source reentry insulation was also varied. Heat source units configured in a planar array parallel to the heat source heat exchanger and in a pincushion array interleaved with the heat source heat exchanger were considered.

E-6105

A PARAMETRIC THERMAL ANALYSIS OF AN ISOTOPE BRAYTON HEAT SOURCE DESIGN DURING STEADY STATE OPERATION

by Raymond K. Burns

Lewis Research Center

E-6105

SUMMARY

A thermal analysis has been performed to predict the internal temperatures, particularly the liner temperature, in an isotope heat source (a design based on Pioneer technology and referred to here as IBHS) during operation in a Brayton power system heat source unit. The heat source temperatures were determined for a range of heat source and heat source heat exchanger emissivities which could be expected, for a range of heat exchanger temperatures around the nominal design for 1600° F turbine inlet temperature, and for a range of heat source fuel load around the nominal value of 400 watts. Heat sources with three types of reentry insulation were considered, namely the nickel-zirconia thermal switch and pyrolytic graphite in two and three layers. Three heat source unit geometries were considered, a planar array of heat sources with heat transfer from one side of the array, a pincushion configuration with heat transfer from two sides of heat source rows, and a limiting case in which individual heat sources were axisymmetrically surrounded by a heat exchanger.

The IBHS design considered in this analysis has a 6.3-inch long capsule and a 400-watt fuel load and either a thermal switch or two layers of pyrolytic graphite reentry insulation (emissivity of 0.8). The results presented show that this heat source is marginal in meeting the assumed steady state temperature limit of 2200° F on the liner when the heat source is in a planar array. For this same heat source, with a thermal switch insulation sleeve, in a pincushion array, it was predicted that the liner temperature would be 130° F lower. For an IBHS with two layers of pyrolytic graphite insulation it was predicted that the liner would be 100° F lower in a pincushion array than in a planar array HSU.

As a comparison to the IBHS, results are also presented for an Isoloaf heat source in which the energy is not constrained to be transferred through reentry insulation during operation. The

liner temperature in an Isoloaf heat source is shown to be much less sensitive to variations in reentry insulation than in the IBHS design. The liner temperature in an Isoloaf heat source with two layers of pyrolytic graphite (emissivity assumed 0.8) in a planar array is shown to be very close to that in the IBHS with the same capsule and insulation but in a pincushion array.

INTRODUCTION

A thermodynamic power system to develop auxiliary electric power in space is being developed by NASA Lewis Research Center. The system operates on a closed loop Brayton cycle (see ref. 1 & 2). One of the energy sources under consideration for this system is the radioisotope Pu-238. The isotope fuel is contained in refractory metal capsules which are surrounded by reentry protection materials. The individual reentry protected capsules are called heat sources (HS) and are assembled onto a support structure for operation with the Brayton system. This assembly is referred to as the heat source unit (HSU). The thermal energy of the radioisotope fuel is radiated from the HSU to the heat source heat exchanger (HSHX). As the Brayton cycle working gas passes through the HSHX it is heated to the 1600° F turbine inlet temperature. In order that the HSU can be easily and safely separated from the power system, without opening the Brayton cycle gas loop, there is no physical contact between the HSU and the HSHX.

Should atmospheric reentry ever occur, the entire HSU is an integral part of a heat source reentry vehicle (HSRV) which is designed for safe, predictable, intact reentry of the HSU (see ref. 3). In addition, should an individual HS become separated from the HSU and HSRV its individual reentry protection materials are intended to provide it with safe reentry capability.

The number of heat sources used in the HSU, the HS fuel load, and the HSU geometry depend on constraints on system size and weight and on operational thermal constraints. The heat source (which is described in more detail later) evaluated in this analysis for use in the Brayton power system HSU is referred to as the Isotope Brayton heat source (IBHS). The IBHS contains a sleeve of reentry insulation for protection of the capsule during individual HS reentry. However, since the thermal energy from the capsule must be transferred through this insulation during power system operation, the presence of the insulation increases operational temperatures of the fuel capsules. When an adequate amount

of insulation is included for reentry protection, it becomes difficult to meet the thermal constraints during power system operation (see ref. 4). The IBHS design is limited in operational temperature by the compatibility of the fuel with the metallic liner surrounding it (this is discussed later).

The conflict between reentry and operational thermal constraints can be alleviated in two ways. One approach would be to change the HS reentry characteristics in order to reduce the required amount and extent of the reentry insulation. A second approach would be to change the thermal boundary conditions on a HS to reduce its operational temperatures.

The main objective of this analyses is to investigate the second alternative. To do this, the operating temperatures of a capsule in an IBHS are predicted for three HSU geometries: (1) a planar array with heat transfer to the HSHX from one side of the array (the present geometry, see ref. 3), (2) an array of heat sources with heat transfer to the HSHX from two sides of the array (representing the pincushion geometry, see ref. 5), (3) a HSHX axisymmetric with an individual HS over its full length (representing the limiting case of maximum heat transfer area). In addition, the HS fuel load, the HSHX temperature, the HS reentry insulation, and the HS and HSHX surface emissivities are varied.

The first alternative mentioned above to alleviate the conflict between reentry and operational thermal constraints has been investigated in a preliminary manner in reference 6. The HS configuration examined there (shown in fig. 1b) was referred to as an Isoloaf HS and is aerodynamically shaped so that if the HS stabilizes during reentry it is in a predetermined orientation. Reentry insulation is included only on the side of the HS designed to lead during any possible stable reentry attitude. Such a configuration eliminates the need to transfer energy through the insulation during power system operation and therefore reduces operational temperatures of the capsule. Some predictions of operational temperatures in an Isoloaf HS are included here as a comparison to the IBHS.

DESCRIPTION OF A HEAT SOURCE

The heat source design (IBHS) examined here is shown in figure 1a. It is a derivative of the HS being developed by the AEC for the Pioneer mission isotope thermoelectric generator. The fuel is contained within a hemispherically capped, cylindrical,

refractory metal capsule. The capsule structural member is a tantalum alloy (T-111) and is separated from the fuel by a tantalum-10% tungsten liner. The liner is intended to prevent reactions between the fuel and the structural member. The T-111 member is covered by a platinum-20% rhodium oxidation resistance clad. The fuel is distributed throughout the cylindrical portion of the capsule with the hemispherical end regions being filled by molybdenum spacers.

A heat source consists of the fueled capsule and its reentry protection. The IBHS reentry protection consists of POCO and Carb-I-Tex graphites and insulating materials. The cylindrical portion of the capsule is surrounded by a sleeve of reentry insulation material. The capsule and insulating materials are held within an outer sleeve of POCO graphite by Carb-I-Tex graphite end plugs. The end plugs are separated from the capsule by tantalum felt compliance pads and a layer of TZM (molybdenum alloy). The exterior shape of the POCO graphite is a hexagonal cylinder.

In the Pioneer application the cylindrical sleeve of reentry insulation currently being considered (see ref. 7) is three layers of pyrolytic graphite (PG) with a total thickness of 200 mils. In the IBHS being evaluated for use with the Brayton power system, two other types of reentry insulation are currently being considered by the AEC. One consists of a sleeve of two layers of PG with total thickness of 133 mils. The other consists of a 200 mil thick sleeve of nickel-zirconia thermal switch material. This material is a zirconia foam impregnated with nickel and exhibits an irreversible decrease in thermal conductivity when the material reaches or exceeds the nickel melting temperature (2600° F) during atmospheric reentry (see ref. 8). The material thus has a desirably low thermal conductivity during reentry and a slightly higher value during power system operation.

The fuel capsule is a vented design. A pressure retention device (PRD) is included in one end of the capsule (not shown in figure 1a) to maintain a helium pressure of 1.0 to 6.0 psia within the platinum-20% rhodium clad. In the present thermal analysis it is assumed that all gaps within the capsule are helium filled.

THERMAL CONSTRAINTS

The temperature distribution within the IBHS located within the HSU array during steady state power system operation must be kept below a limit which is determined by the compatibility of

the fuel with the liner material. For the purpose of the present thermal analysis, this upper limit is assumed to be 2200° F. The validity of this limit has yet to be confirmed by test data.

A second thermal constraint applies to atmospheric reentry of an individual HS. It is presently required that the platinum-20% rhodium oxidation resistance clad on the capsule be kept below its melting temperature (~3400° F). A number of stable orientations and tumbling and spinning motions during reentry must be considered in the selection of the HS reentry protection materials. It has generally been accepted that the side-on-stable orientation throughout the trajectory is the most severe thermally. During side-on-stable reentry of an IBHS, in an orbital decay trajectory, the peak temperature of the POCO graphite is predicted to reach about 4000° F (see ref. 4 & 9). This, together with the high thermal conductivity of POCO (~20 BTU/hr-ft-°F), results in the necessity of including a layer of insulation between the POCO and the clad, to keep the clad below its melting temperature during side-on-stable reentry. Because of the omnidirectional reentry characteristics of the IBHS (it could stabilize with any of the six sides leading) this insulation must surround the capsule as shown in figure 1.

Because the insulation surrounds the capsule, the thermal energy from the fuel must be transferred through it during steady state power system operation. Including the insulation in the IBHS raises its steady state liner temperature resulting in a conflict between the steady state and reentry thermal constraints. This is further discussed in reference 4. The amount of insulation required depends on the trajectory, as well as on the HS orientation during reentry, and on the temperature distribution in the HS at the beginning of the trajectory. As shown in reference 4, if an adequate amount of insulation is included in an IBHS to protect the clad during side-on-stable reentry, the steady state temperatures may exceed the assumed acceptable limit.

The amount of insulation necessary for a tumbling or spinning HS is much less than required for a side-on-stable orientation (e.g., see ref. 4). Therefore a possible way to avoid the conflict between the two thermal constraints would be to eliminate the possibility of side-on-stable orientation occurring so that the insulation requirements are reduced. Another approach would be to aerodynamically shape the HS for predictable orientation and then to include insulation only on the side of the HS designed

to lead if the HS attitude stabilized during reentry. The opposite side could be used as a heat transfer path during steady state power system operation. This approach has been examined in reference 6. A third approach would be to accept the amount of insulation required for reentry and to reduce steady state operational temperatures by other means, as examined in this analysis.

ANALYSIS

The IBHS considered in this analysis is shown in figure 1a. The temperatures of the heat source are predicted for three HSU configurations. One is the close-packed planar array of heat sources which radiate energy to the HSHX from only one side of the array (fig. 2a). This corresponds to the present HSU design approach (ref. 3). Another case considered is a close-packed array of heat sources which radiate energy to the HSHX from both sides of the array. Physically this case could be approached by arranging the heat sources in single rows with the heat source ends attached to the HSU support plate. The HSHX would then be inserted between rows of heat sources so that each HS row radiated energy to the HSHX on two opposite sides of the row (see fig. 2b). This is the pincushion HSU configuration considered in reference 5. In both of these cases it was assumed that there is no space between adjacent heat sources. Finally, the third case considered is the HSHX axisymmetrically surrounding individual heat sources over their full length. This is the limiting case representing the maximum heat transfer area between HS and HSHX.

The present analysis is divided into two parts. First, a preliminary estimate of the HS radiating surface temperature was made as a function of the emissivities of the HS exterior surface and the HSHX surface and as a function of the sink temperature for the three HSU geometries listed above. A simple one dimensional model of the radiative transfer between the HS and HSHX was used for this purpose. The results give an indication of the sensitivity of the HS temperatures to these factors. This approach avoids the detailed consideration of the heat transfer within a HS with considerable savings in computational time and effort.

This simple model does not however predict the actual variation in temperature over the HS surface or the temperature difference between the HS surface and the liner hot spot. The liner hot spot

is the operating temperature of primary interest and the difference between this temperature and the HS surface temperature is actually a function of such parameters as HSU geometry, HS fuel load, and sink temperature. The second part of this analysis was to examine the HS interior heat transfer in detail. Two thermal models were used for this purpose, a one-dimensional model for the axisymmetric HS, HSHX case and a three-dimensional model for the other two HSU geometries considered.

One Dimensional Radiation Transfer Thermal Model

The one-dimensional thermal model used to simulate the radiative exchange between the HS array and the HSHX is shown in figure 3. Possible temperature variations over the HS surface and over the HSHX surface are neglected. The HSHX is assumed to be an infinite plane surface. The HS array surface is taken to be infinite with parallel, 120 degree included angle V-grooves representing the top surface of the heat sources. The resulting temperature of the HS surface can be thought of as an average of the actual temperature variation which would occur.

The radiative flux input to the HSHX for the one-dimensional model in figure 1 can be written:

$$q_{HX} = \frac{\epsilon_{HS}\epsilon_{HX}\left(\sigma T_{HS}^4 - \sigma T_{HX}^4\right)}{1 - \rho_{HS}F_{HS-HS} - \rho_{HS}\rho_{HX}F_{HS-HX}} \tag{1}$$

(a symbol list is included in Appendix A).

For the two HSU geometries considered in which the heat sources are arranged in a planar array or in rows, the view factors are

$$F_{HS-HX} = 0.866$$
$$\text{and } F_{HS-HS} = 1-F_{HS-HX} = 0.134. \tag{2a}$$

For the case in which it is assumed that the HSHX surrounds each HS axisymmetrically the view factors are

$$F_{HS-HX} = 1.0$$
$$\text{and } F_{HS-HS} = 0.0. \tag{2b}$$

For this model, the radiative flux input to the heat exchanger is also equal to the HS fuel load divided by the projected area of a HS on the HSHX:

$$q_{HX} = \frac{Q_{HS}}{A_{HX}} \tag{3}$$

Equations (1) - (3) are solved to obtain the HS radiating surface temperature as a function of the HSHX temperature and the HS and HSHX emissivities.

Axisymmetric, One-Dimensional Thermal Model of a Heat Source

In order to determine HS interior temperatures, a more detailed thermal model is required. Of the three HSU geometries considered, the axisymmetric HSHX case is most easily handled. If the effect of the corners on the hexagonal shaped POCO are neglected, the HS is isothermal in the direction around its axis. In addition, if it is assumed that each element of the HS has no longitudinal temperature gradient, the problem becomes a one-dimensional one, with heat transfer only in the radial direction. This thermal model is shown in figure 4. It can be seen that the possible heat flow path through the hemispherical end of the capsule and the Carb-I-Tex end plug of the HS are not included in the model. Neglect of this possible heat transfer path makes the model conservative (the amount of conservatism will be discussed later). It is assumed that each gap within the capsule clad is helium filled.

Using the one-dimensional HS model in figure 4, the radial temperature distribution in the IBHS was calculated. The temperature change across each element of the HS and across each helium gap was obtained by solving:

$$Q_{HS} = \frac{2\pi k L (T_i - T_o)}{\ln\left(\frac{r_o}{r_i}\right)} \tag{4}$$

where k is the thermal conductivity of the material and L is the logitudinal length of the element in the thermal model. The longitudinal length of the POCO is taken as the overall IBHS length; the length of the insulation sleeve is taken as its actual length; and the length of each element of the capsule is taken as the length of the cylindrical portion of the capsule. It is assumed that heat transfer between the layers of reentry protection materials is by radiation only. The temperature difference across these radiation gaps was determined using:

$$Q_{HS} = \frac{2\pi r_i L (\sigma T_i^4 - \sigma T_o^4)}{\left(\frac{1}{\epsilon_i} + \frac{1}{\epsilon_o} - 1\right)} \qquad (5)$$

Three-Dimensional Thermal Model of a Heat Source

For the other two HSU geometries considered, the HS is not thermally axisymmetric and a multi-dimensional thermal model is required. The model shown in figure 4 was generalized to obtain the three-dimensional thermal model shown in figure 5a. Again the possible heat transfer path through the hemispherical ends of the capsule and the Carb-I-Tex end plugs are not included so the model is conservative. The degree of conservatism is not large since the heat transfer path neglected is in fact a high resistance path (the amount of conservatism is evaluated later). As shown by figure 1, this heat transfer path includes the layer of low thermal conductivity tantalum felt. The network of nodes in figure 5a represents one-quarter of an IBHS and was used to obtain the temperature distribution using the CINDA-3G computer code (ref. 10).

The thermal boundary conditions placed on the exterior surfaces of the POCO nodes in the model depend on the particular HSU geometry being considered. The HS was assumed to radiate to a HSHX on one side of the HS array for the planar array HSU and to a HSHX on two opposite sides of a HS row for the pincushion HSU. The radiative exchange factors from the HS surface nodes to the HSHX were calculated including the presence of the adjacent heat sources. The nonradiating exterior surfaces of the HS were assumed to be adiabatic.

The thermal properties of the nodes in figure 5a denoted as reentry insulation were taken to be those of either the nickel-zirconia thermal switch or of pyrolytic graphite (PG). The

thermal switch was taken to be one layer, 200 mils thick radially with a steady state thermal conductivity of 1.5 BTU/hr-ft-^{o}F and a surface emissivty of 0.60. The PG was taken as two separate layers, each 67 mils thick radially, with a thermal conductivity of 0.77 BTU/hr-ft-^{o}F in the radial direction and 120.0 BTU/hr-ft-^{o}F in the circumferential and longitudinal directions. Two values of emissivity were considered for PG, 0.5 and 0.8, because of the uncertainty in the correct value.

The thermal model used for the Isoloaf HS results presented here is shown in figure 5b. It differs from the IBHS model in figure 5a only in the exterior shape of the POCO and in the extent of the reentry insulation. During power system operation, the Isoloaf heat sources are assumed to be arranged in a planar array with the flat side resting on the HSU support plate. The thermal energy is transferred from the opposite side to the HSHX. The reentry insulation extends around the capsule only on the flat side of the heat source which is intended to lead if stabilized orientation occurs during individual HS reentry (see ref. 6).

RESULTS OF ANALYSIS

One-Dimensional Radiation Transfer Analysis

In figure 6 the HS radiating surface temperature is shown for the planar array HSU as a function of HS and HSHX emissivities. The HSHX was assumed to be at 1670^{o} F, (hot spot temperature) calculated in reference 3 for a 1600^{o} F turbine inlet gas temperature. As already stated this present calculation neglects possible variations in temperature over the HS surface and results in an average HS surface temperature. For comparison, in figure 7 some HS surface temperatures calculated using a three-dimensional thermal analysis of a complete IBHS are shown. The three-dimensional analysis included detailed consideration of the heat transfer within an IBHS located in the HSU array and radiating to a 1670^{o} F HSHX. The thermal model used for the IBHS was similar to that shown in figure 5 but included the capsule hemispherical end and the Carb-I-Tex end plug. The HS surface emissivity was taken as 0.80 and the HSHX emissivity was taken as 0.85. For these same emissivity values, the one-dimensional model gives a HS surface temperature, as shown in figure 6, of 1814^{o} F. The results given in figure 6 are intended to show the dependence of the HS surface temperature on the surface emissivities. The emissivity of the POCO graphite HS surface is in the range from 0.75 to 0.85. The coatings currently being considered for the HSHX surface range in the emissivities from 0.65 to 0.95.

The steady state thermal analyses performed for the Brayton HSU in references 4, 6, and 9 have assumed an emissivity of 0.80 for the HS and 0.85 for the HSHX. Reference to figure 6 shows that these emissivities ($\epsilon_{HS} = 0.80, \epsilon_{HX} = 0.85$) result in a HS surface temperature 38^{o} F higher than the case where both surfaces are optically black. For the worst combination of emissivities in the ranges mentioned above ($\epsilon_{HS} = 0.75, \epsilon_{HX} = 0.65$) the HS surface is 78^{o} F hotter than the black surface case.

In figures 8 and 9 the average HS radiating surface temperature obtained using the one-dimensional model is given as a function of the sink temperature and of HS and HSHX emissivities for the planar array HSU, for the pincusion HSU, and for the HSHX axisymmetric with each HS. The emissivities examined in these figures are values which are in the expected ranges. It is seen that the HS surface temperature is more sensitive to emissivities for the planar HSU than for the other HSU geometries which have larger heat transfer areas.

Figures 8 and 9 also show the dependence of the HS surface temperature on sink temperature for the three HSU geometries considered. The change in HS surface temperature per degree of change in the sink temperature is slightly different for the three HSU geometries considered. As expected, this rate of change is less for the planar array HSU for which the HS temperatures are highest. The sink temperature (the HSHX temperature) is a function of the Brayton working gas temperature and the HSHX design. For a given HSHX design, the sink temperature for the HSU is reduced by reducing the turbine inlet gas temperature. For the present HSHX design the HSHX hot spot was calculated to be 1670^{o} F for a 1600^{o} F turbine inlet gas temperature (ref. 3). It is expected that a decrease in heat exchanger temperature (sink temperature) would be slightly less than the corresponding decrease in turbine inlet temperature.

The HS radiating area for the pincushion HSU is assumed to be twice the area for the planar array HSU. In figure 9 for a HSHX emissivity of 0.9 and a sink temperature of 1670^{o} F, the HS surface temperature for the pincushion HSU is 66^{o} F less than for the planar array HSU. The HS surface temperatures for the pincushion HSU are seen to be approaching the limiting case in which the HSHX is axisymmetric with the HS. In figure 9 for $\epsilon_{HX} = 0.9$ and $T_{HX} = 1670^{o}$ F, the difference in HS surface temperature between the pincushion HSU and the axisymmetric case is only 24^{o} F.

Figures 6, 8, and 9 which show the effects of surface emissivities, sink temperature and HSU geometry on the HS radiating surface temperature are an indication of the corresponding effect on the liner hot spot temperature. However, the actual temperature difference between the liner hot spot and HS surface is a function of many factors. Some of which are temperature level, HS design (such as the type of reentry insulation sleeve), HS fuel load, and HSU design. Therefore, quantitative conclusions about the direct effect of surface emissivities, sink temperature and HSU design on the liner temperature must be drawn carefully from the data in these figures. For example, the difference in liner hot spot temperature between the planar array HSU and the pincushion HSU should be greater than the difference indicated in figures 8 and 9 because the circumferential temperature change within a HS would be less for the two-sided heat transfer case (pincushion HSU) than for the one-sided heat transfer case (the planar array HSU). Examination of these effects requires a thermal analysis of the HS interior which is the next step in the present analysis.

Axisymmetrical Heat Source Thermal Analysis

The HS interior temperatures are most easily determined for the case in which the HSHX is axisymmetric with the HS. Using the thermal model in figure 4, which neglects longitudinal temperature variations, the radial temperature distribution can easily be determined. This model was used to determine the IBHS interior temperature distribution as a function of sink temperature for heat sources having several different kinds of reentry insulation sleeves.

The reentry insulation sleeves considered were the nickel-zirconia thermal switch, two layers of PG (which are being evaluated for use in the HS for the Brayton isotope power system) and three layers of PG (which is being evaluated for use in the HS for the Pioneer mission). The IBHS temperatures for these cases are given as a function of sink temperature, for a 400 watt fuel load, in figures 10 through 14. The emissivity for the HS exterior surface and the HSHX surface were taken as 0.80 and 0.85 respectively. One point made clear by figures 10 through 14 is that the radiation gaps assumed to exist between separate layers of the reentry protection materials are a significant thermal penalty during power system operation. In all cases considered,

the temperature difference across the radiation gaps formed by including the insulation sleeve are greater than the temperature change across the insulation. For analysis at steady state operation, the insulation surface emissivity is as important a parameter as the thermal conductivity of the insulation. This can be seen by comparing figures 13 and 14 for two different insulation emissivities. The temperature differences across all of the gaps within the capsule clad, assumed to be helium filled, are predicted to be within the range of 20 to 30° F for the cases in figures 10 through 14.

In figure 15, the liner temperatures for heat sources with these types of reentry insulations are compared. It is seen that only two cases, the thermal switch and two layers of PG with a 0.80 emissivity, are below the assumed maximum liner temperature of 2200° F. Although this thermal model is conservative in that the heat transfer path through the capsule end is neglected (the amount of conservatism in this assumption will be discussed later) it also assumes the maximum possible heat transfer area (i.e., HSHX axisymmetric to the HS). Even in this limiting case of maximum heat transfer area, the results indicate that three layers of PG would produce liner temperatures above the assumed limit for HS fuel load of 400 watts and sink temperatures of interest.

The axisymmetric HS thermal analysis is of interest because it is a limiting case of maximum possible heat transfer area. But to determine the liner hot spot temperature for a physically realistic case in which there would be a circumferential temperature gradient, a more general thermal model is required.

Three-Dimensional Heat Source Thermal Analysis

In order to examine the HS interior temperatures as a function of sink temperature and HS fuel load for the planar array HSU and the pincushion HSU, the axisymmetrical IBHS thermal model was generalized to the three-dimensional model in figure 5a. This model was used to determine the liner hot spot temperature in an IBHS with two types of reentry insulation, nickel-zirconia thermal switch and two layers of PG. The results are given in figures 16 through 18 for a 400-watt HS fuel load as a function of sink temperature. For reference, some results of the axisymmetric IBHS analysis are included. Emissivities of 0.80 and 0.85 on the HS exterior surface and on the HSHX surface respectively are again used.

As noted earlier, the HS thermal models used in this analysis are conservative in that they neglect the possible heat transfer path through the capsule ends and the Carb-I-Tex end plugs. An estimate of the degree of conservatism can be obtained by comparing the liner hot spot temperature predicted using the present thermal model to that predicted using a model which includes the capsule end region and Carb-I-Tex end plug. Results have been obtained using such a complete three-dimensional model for an IBHS containing a nickel-zirconia thermal switch. For a sink temperature of 1670° F the results of figure 16 were shown to be conservative (hotter) by 70° F for the planar array HSU and by 65° F for the pincushion HSU. Since the amount of conservatism was found to be relatively constant for the cases considered it was felt that use of the present thermal model for this analysis was justified. The present results can be used for example to make a valid comparison between HS and HSU designs but the conservatism must be considered if the absolute temperature level is to be compared to the acceptable limits.

Comparing the liner hot spot temperature for the planar array HSU for an IBHS with a thermal switch in figure 16 to that for an IBHS with two layers of PG (with $\epsilon_{PG} = 0.80$) in figure 17 shows that the two temperatures are close. The liner temperature for the thermal switch case is 17° F lower than the PG case at a 1700° F sink temperature and 29° F lower at a 1500° F sink temperature. Figures 16 and 17 show that the thermal advantage in changing the HSU configuration from the planar array to the pincushion is greater for an IBHS with a thermal switch than an IBHS with two layers of PG. For a sink temperature of 1670° F the difference in liner hot spot between the planar array HSU (one-sided heat transfer) and the pincushion HSU (two-sided heat transfer) is 130° F for an IBHS with a thermal switch and 100° F for an IBHS with two layers of PG. This is the result of the higher circumferential thermal conductivity of PG.

In figure 18, the liner hot spot temperature is given for an IBHS with two layers of PG assuming the PG emissivity is 0.50 rather than the PG emissivity of 0.80 assumed in figure 17. These two values were used because of the present uncertainty in the correct value. Comparison of figures 17 and 18 again points out the importance of the thermal penalty of the assumed radiation gaps between layers of reentry protection materials. The results in figure 18 for $\epsilon_{PG} = 0.50$ show liner hot spot temperatures well above the assumed upper limit of 2200° F.

Up to this point the HS fuel load has been held constant at 400 watts. The variation in liner hot spot temperature with change in IBHS fuel load is shown in figures 19 through 21 for heat sources with a thermal switch and with two layers of PG reentry insulation. The sink temperature was taken as 1670° F in these figures. An increase in IBHS fuel load increases the circumferential heat transfer and, therefore temperature gradient, resulting in a larger difference between the planar array HSU and the pincushion HSU.

The results presented so far show the effects of some of the heat source system parameters on the operational temperature of an IBHS. Variation of these parameters to reduce operational temperatures is one possible approach to alleviating the conflict between operational and reentry thermal requirements. Another approach, mentioned in the Thermal Constraints section, is to aerodynamically shape the HS in order to eliminate the need for insulation completely surrounding the capsule. One possible configuration to accomplish this, the Isoloaf HS, was examined in reference 6 using a two-dimensional thermal analysis. Some results obtained for the Isoloaf HS using a three-dimensional model similar to the one used here for an IBHS are presented in figure 22. They are compared with the IBHS in a planar array and the IBHS in a pincushion array HSU.

The Isoloaf HS thermal model is shown in figure 5b. As discussed in reference 6, the shape is intended to make the HS have only one stable attitude (i.e., flat side leading, side-on orientation). The reentry insulation surrounds the capsule only on the flat side. During power system operation the Isoloaf heat sources are arranged in a planar array with the flat side on the support plate. The thermal energy of the capsule is transferred toward the HSHX through the uninsulated side.

In figure 22, the Isoloaf HS results are for two layers of PG reentry insulation, the same amount used for the IBHS results given. It is seen that although the Isoloaf HS results are for a planar array HSU the liner hot spot temperature is lower than it would be in an IBHS using the more complicated pincushion HSU. The Isoloaf HS results are also shown to be insensitive to slight changes in the properties of the insulation. For the IBHS with PG emissivity of 0.5, the liner hot spot temperature exceeds the assumed upper limit of 2200° F for a 400-watt fuel load (even if the conservatism of the present three-dimensional thermal model is taken into consideration). However, the liner hot spot

temperature in the Isoloaf HS with a PG emissivity of 0.5 is below the temperature limit for a 400 watt-fuel load (especially if the conservatism is considered) being relatively unaffected by the value.

CONCLUDING REMARKS

The heat source operating temperatures are a function of the fuel load, the HSU geometry, the sink temperature (HSHX temperature and therefore turbine inlet temperature) and the HS reentry insulation. This combination must be such that the liner operational temperature is below the maximum allowable limit assumed at 2200° F. IBHS reentry thermal requirements make it necessary to include a reentry insulation sleeve between the capsule and the POCO graphite. Since including this insulation significantly increases operational temperatures within the capsule, a conflict arises between reentry and steady state thermal constraints. This conflict can be alleviated by varying the above mentioned parameters in order to reduce the HS operational temperatures.

The results for an IBHS with dimensions given in figure 1, show:

1. For a planar array HSU the average surface temperature of the hottest HS for the worst expected combination of HS and HSHX surface emissivities ($\epsilon_{HS} = 0.75$, $\epsilon_{HX} = 0.65$) was predicted to be 40° F hotter than for the nominal case ($\epsilon_{HS} = 0.8$, $\epsilon_{HX} = 0.85$).

2. In a planar array, the HS surface temperatures are more sensitive to HS and HSHX surface emissivities than in a pincushion array.

3. For the IBHS considered in this analysis using a thermal switch insulation and having a 400-watt fuel load and a sink temperature of 1670° F, the liner hot spot temperature in a HS in a planar array was predicted to be 130° F hotter than for one in a pincushion array. If two layers of PG ($\epsilon_{PG} = 0.8$) insulation is used in the IBHS, the results predicted the HS liner hot spot to be 100° F hotter for the planar array than for the pincushion array HSU.

4. The liner hot spot temperature in the IBHS considered, in a planar array HSU, is about the same with either a thermal switch insulation sleeve or with two layers of PG ($\epsilon_{PG} = 0.8$) insulation. Taking into consideration the conservatism of the thermal model used, (70° F for an IBHS with thermal switch insulation and located in a planar array HSU) both cases were predicted to be marginal in being able to operate below the assumed 2200° F temperature limit on the liner.

5. The radiation gaps assumed to exist between separate layers of the reentry protection materials are a significant thermal penalty during power system operation. As a result, the emissivity of the surfaces of the reentry protection materials is as significant a parameter as the thermal conductivity of the materials.

6. The liner temperature in the IBHS with three layers of PG insulation and 400-watt fuel load was shown to exceed the assumed maximum liner temperature of 2200° F even for the case in which the HSHX is axisymmetric with the HS.

7. The liner hot spot temperature in an Isoloaf HS (a variation in HS configuration) in a planar array was predicted to be lower than in an IBHS of same length and fuel load in a pincushion array. The Isoloaf temperatures were also shown to be relatively insensitive to the amount and type of reentry insulation used.

APPENDIX A. NOMENCLATURE

A	Area
F_{ij}	Geometric view factor from i to j
HS	Heat Source; metallic capsule containing isotope fuel surrounded by individual reentry protection materials.
HSU	Heat Source Unit; array of heat sources and its supporting structure for use as Brayton engine energy source.
HSHX	Heat Source Heat Exchanger
HSRV	Heat Source Reentry Vehicle; reentry protection for the heat source unit.
IBHS	Isotope Brayton Heat Source; design based on the Pioneer mission thermoelectric generator heat source.
k	Thermal conductivity
L	Length
POCO	POCO graphite reentry material of a heat source.
PG	Pyrolytic graphite
Q	Heat source fuel load
q	Heat flux
r	Radius
T	Temperature
T-111	Tantalum alloy strength member of a capsule.
ϵ	Emissivity
ρ	Reflectivity

Subscripts:

HS	refers to heat source
HX	refers to heat exchanger
INS	refers to reentry insulation material
i	refers to inside surface
o	refers to outside surface
PG	refers to pyrolytic graphite

REFERENCES

1. Brown, William J.: Brayton-B Power System - A Progress Report. Proceedings of the 4th Intersociety Energy Conversion Engineering Conference. AIChE, 1969, pp. 652-658.

2. Klann, John L.: Steady-State Analysis of a Brayton Space Power System. NASA TN D-5673, 1970.

3. Ryan, Richard L.; and Graham, John W.: Isotope Reentry Vehicle Design Study, Preliminary Design: Phase II. Rep. AVSD-0306-69-RR, AVCO Corp. (NASA CR-72555), Aug. 1969.

4. Burns, Raymond: Preliminary Analysis to Determine the Reentry Insulation Requirements on a Pioneer-Type Heat Source for Use in the Isotope Brayton Application. NASA TM X-52850, 1970.

5. Anon.: Isotope Reentry Vehicle Design Study, Conceptual Design, Phase IB, Topical Report. Rep. AVSD-0193-68-CR, AVCO Corp. (NASA CR-72463), Oct. 1968.

6. Burns, Raymond: Preliminary Thermal Analysis of an Aerodynamically Shaped Heat Source for Use with the Isotope Brayton Space Power System. NASA TM X-52891, 1970.

7. Ramon, S.: Steady-State Operating Temperatures of SNAP-19 Pioneer Heat Source. MEMO. SN 19-SR-210, Teledyne Isotopes, Inc., 1970.

8. Anon.: High-Temperature Metal Thermal Switch Development Program First Quarterly Report, July-August 1969. Hittman Associates, Inc., Mar. 1970. (Work under contract AT (29-2)-2797.)

9. Cropp, L. O.: Two-Dimensional Steady-State Operational Thermal Analysis of the Isotope Brayton Heat Source. Rep. SC-RR-70-451, Sandia Lab., Aug. 1970.

10. Lewis, D. R.; Gaski, J. D.; and Thompson, L. R.: Chrysler Improved Numerical Differencing Analyzer for 3rd-Generation Computers. Rep. TN-AP-67-287, Chrysler Corp. (NASA CR-99595), Oct. 20, 1967.

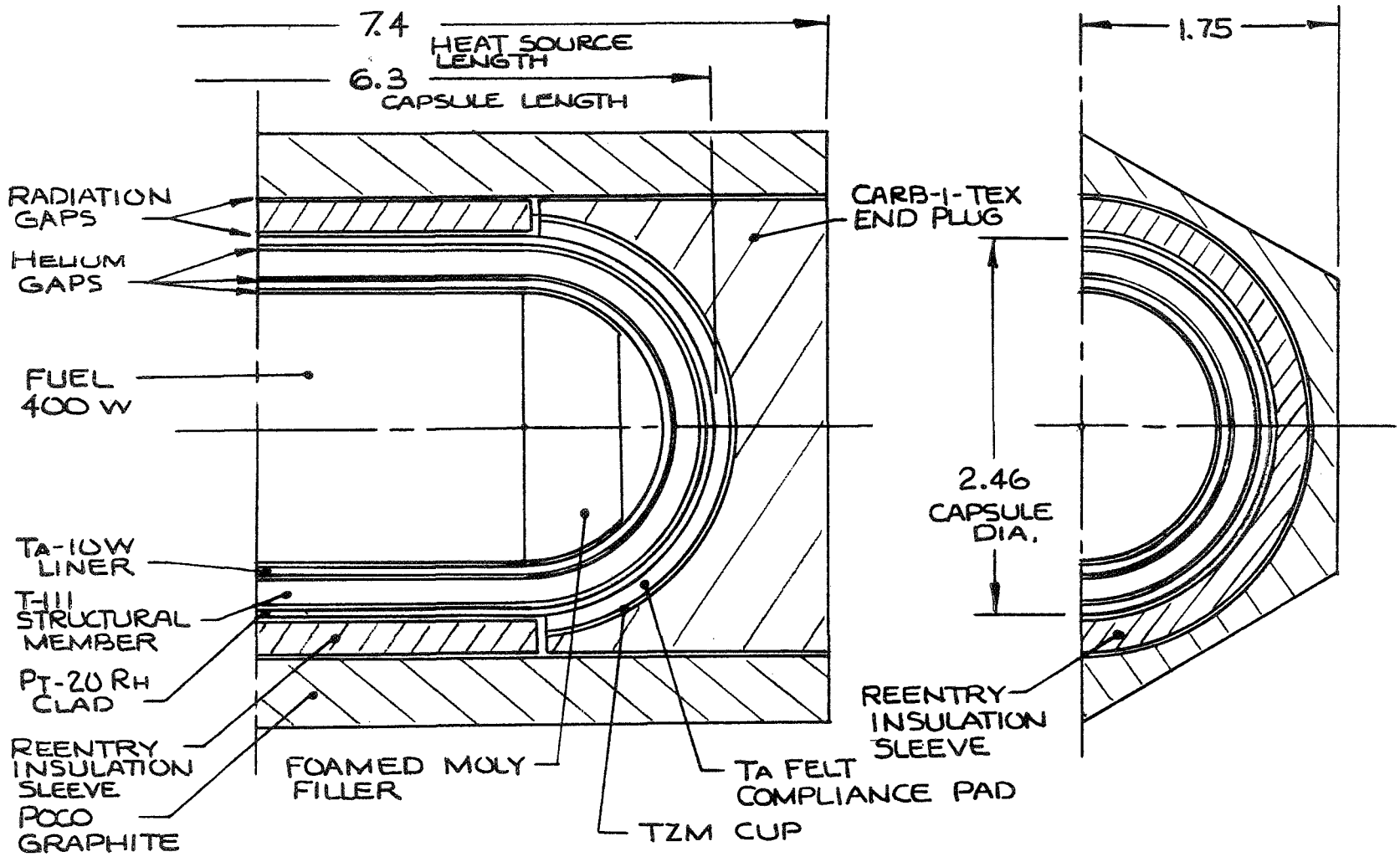

FIGURE 1a SKETCH OF ISOTOPE BRAYTON HEAT SOURCE

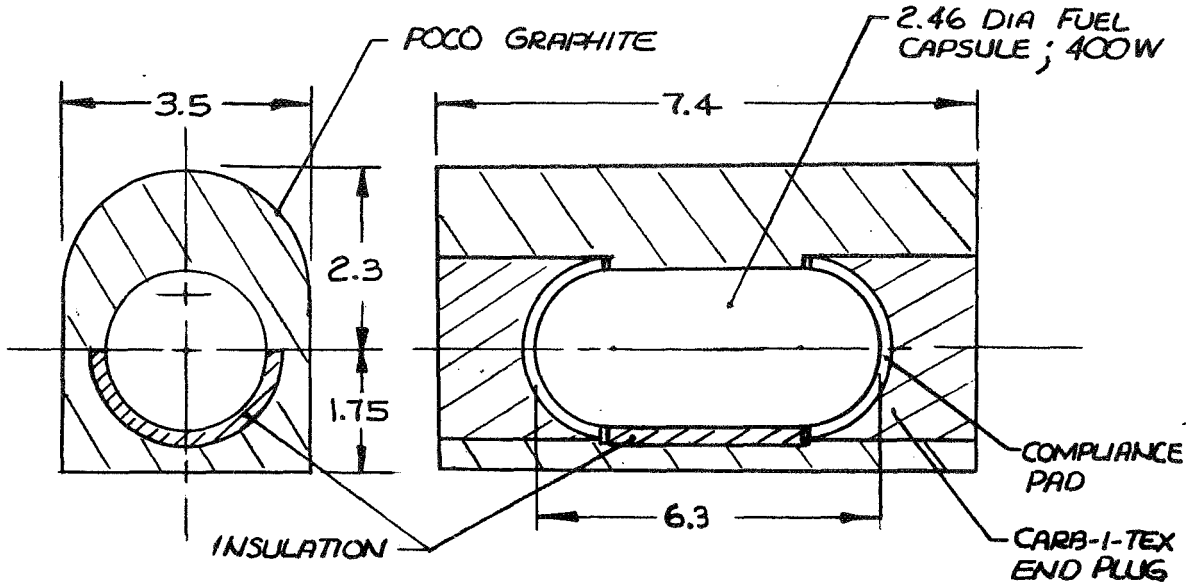

ISOLOAF

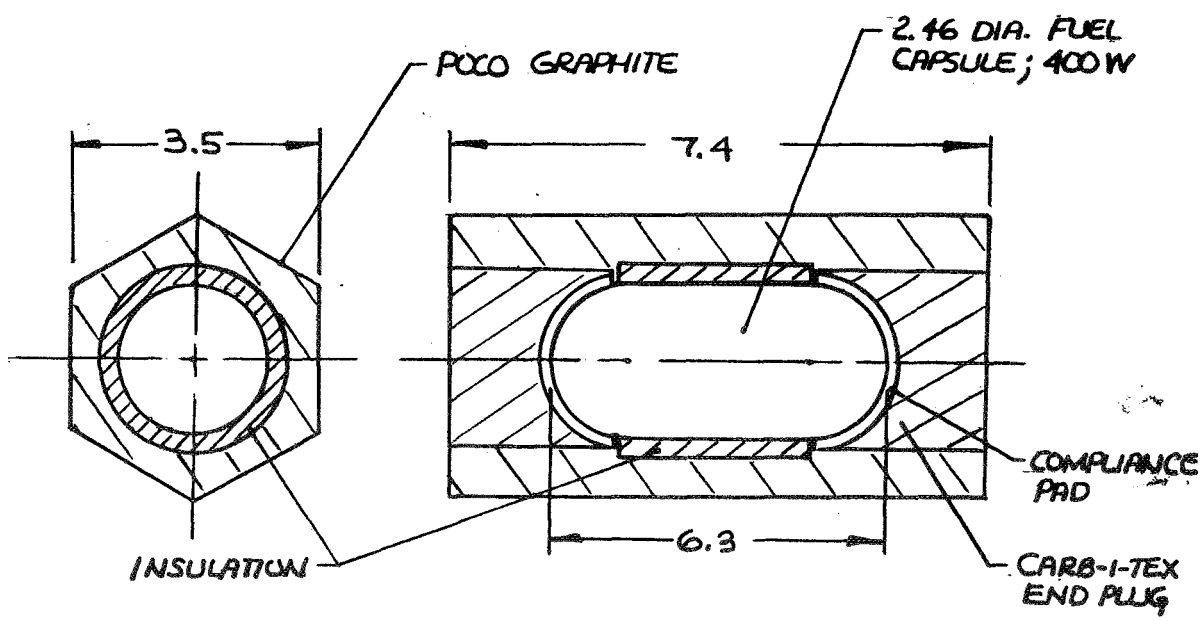

IBHS

FIGURE 1b COMPARISON OF IBHS AND ISOLOAF HS

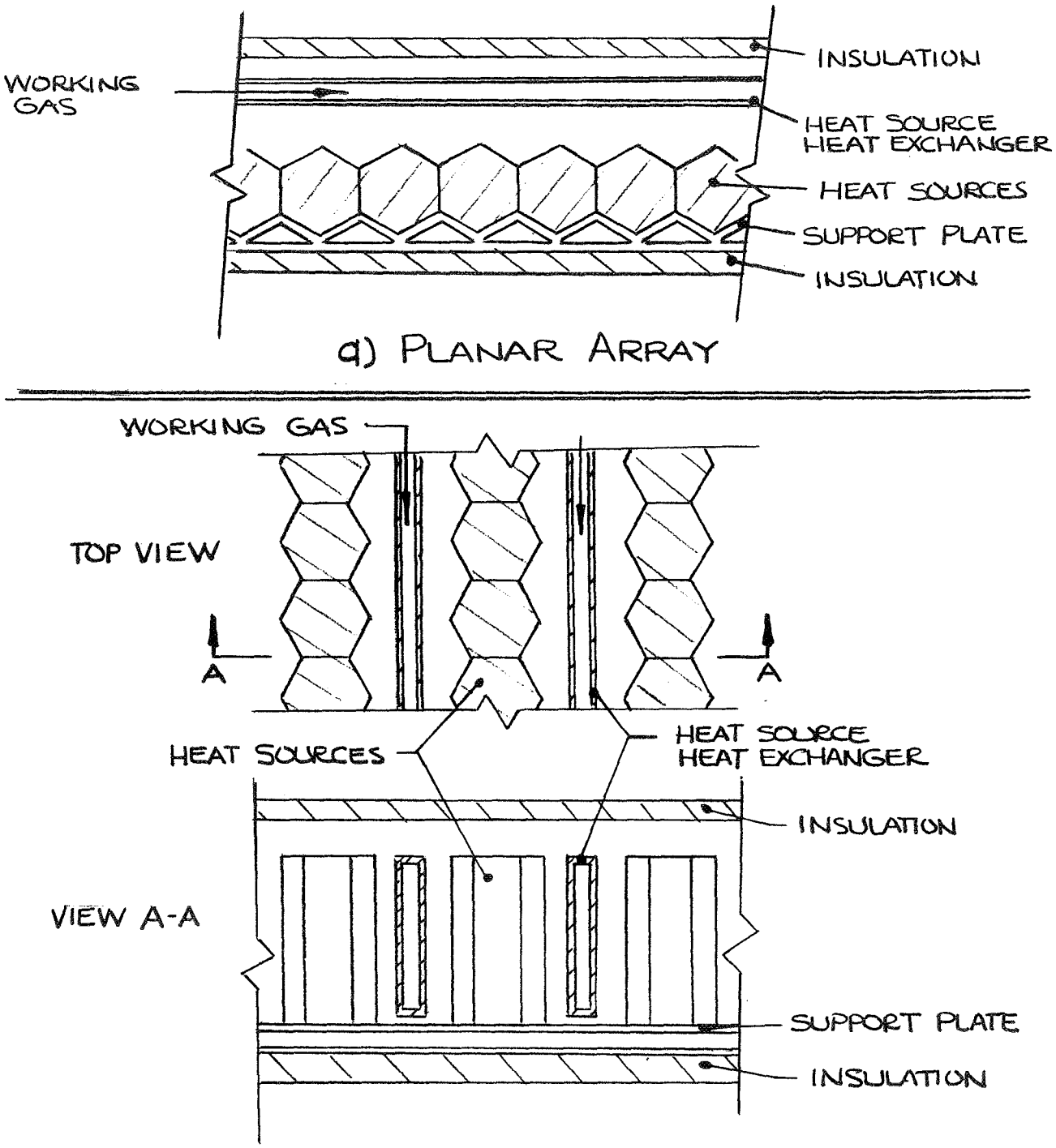

FIGURE 2 SKETCH OF HEAT SOURCE UNIT CONFIGURATIONS

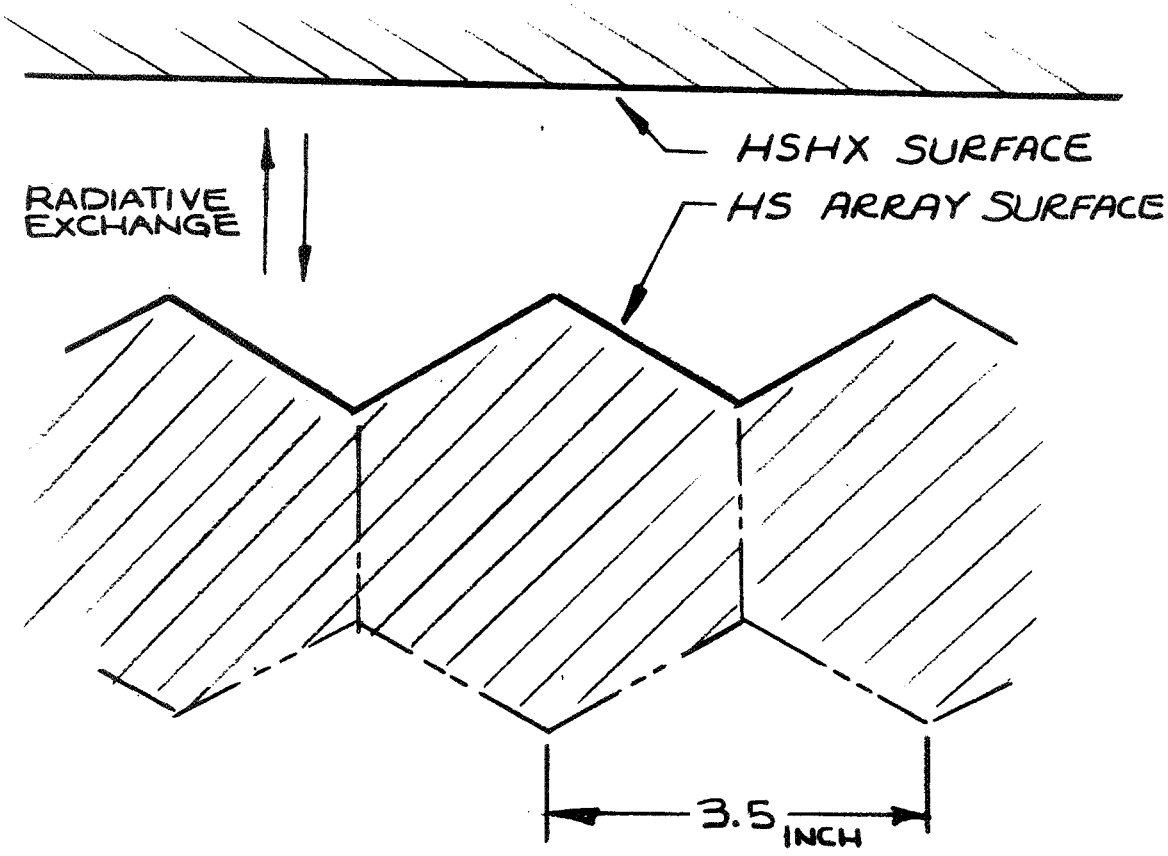

FIGURE 3 ONE DIMENSIONAL RADIATION TRANSFER MODEL

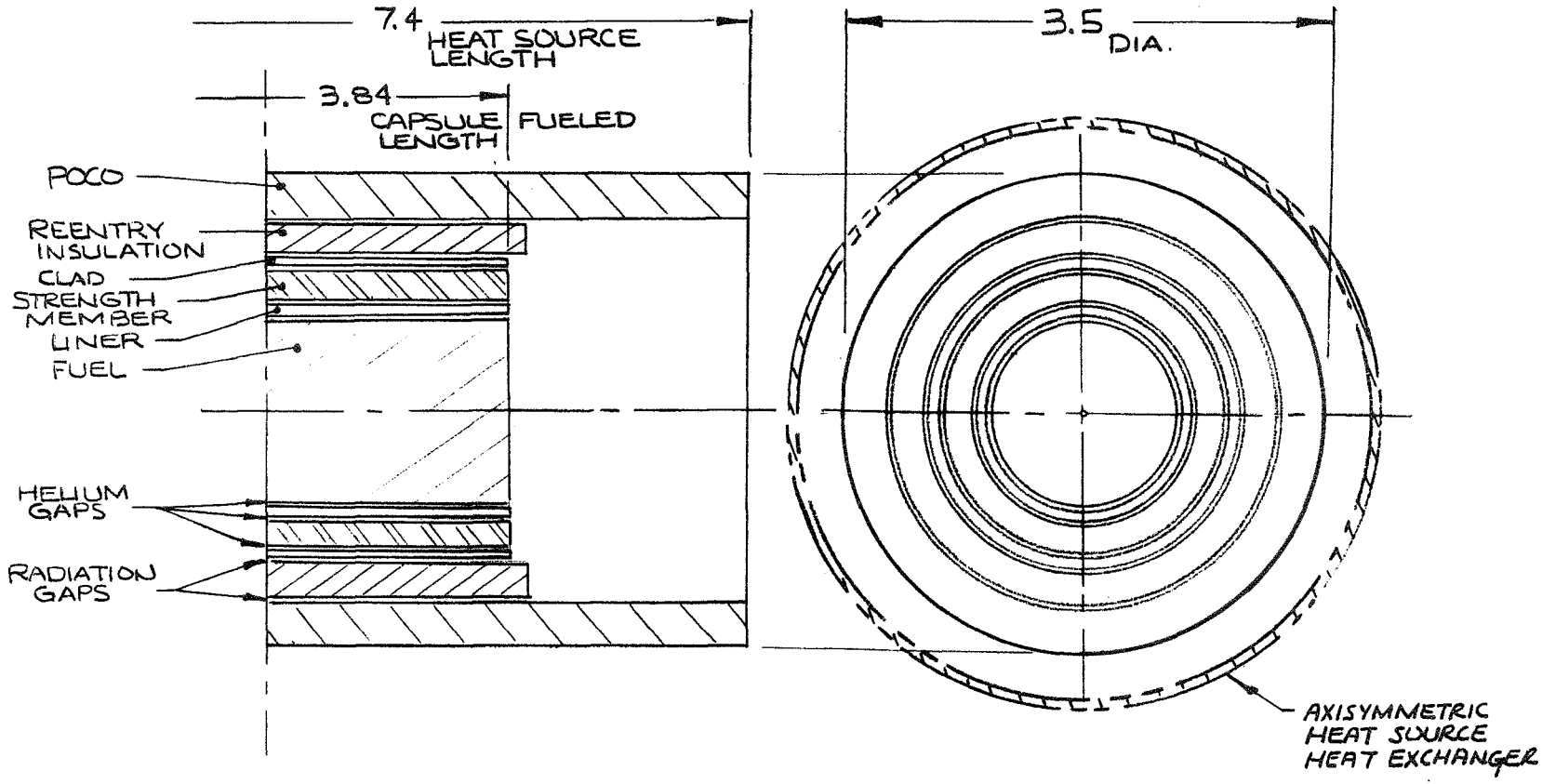

FIGURE 4 AXISYMMETRIC THERMAL MODEL OF AN IBHS

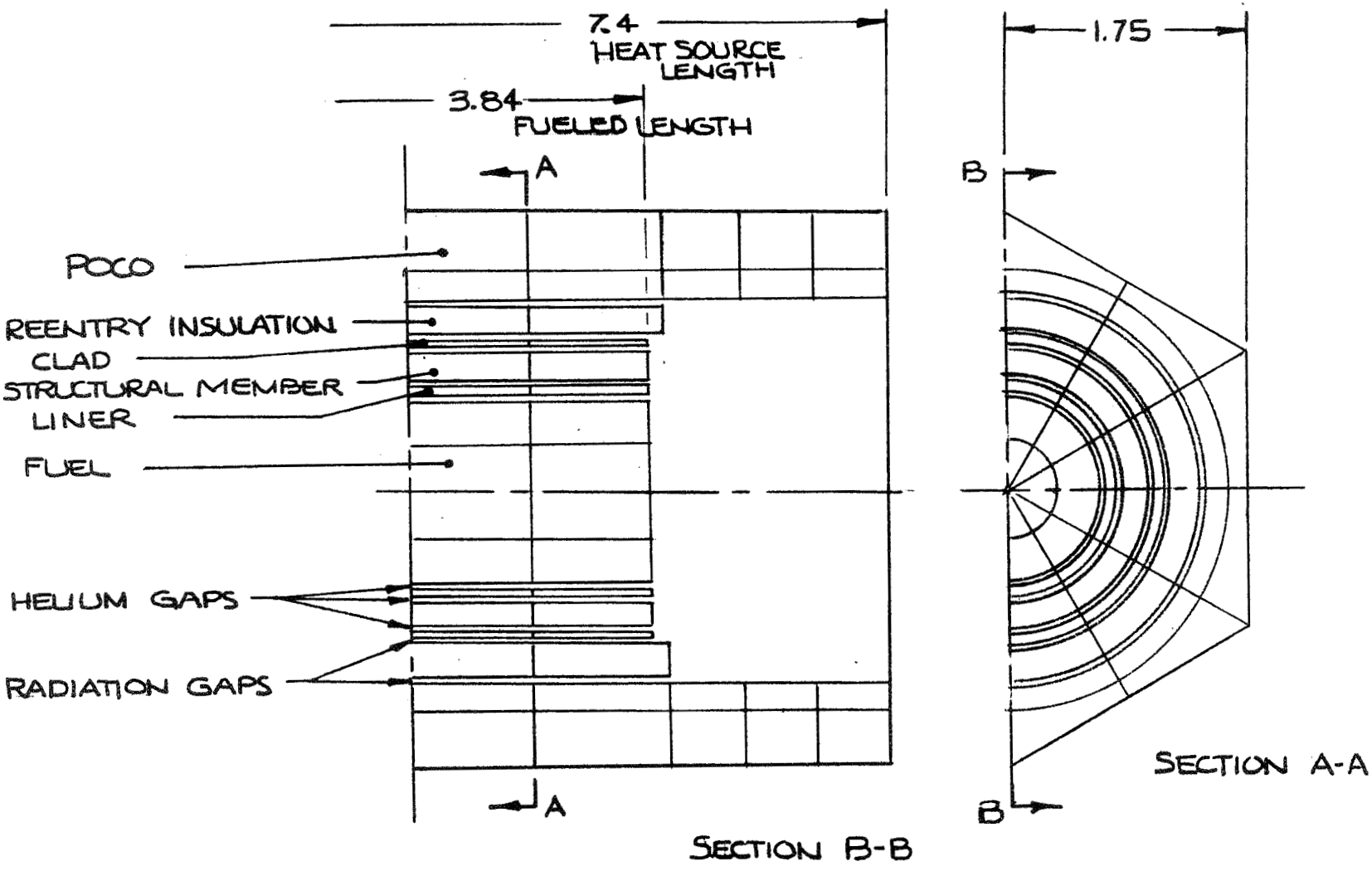

FIGURE 5a THREE DIMENSIONAL THERMAL MODEL OF AN IBHS

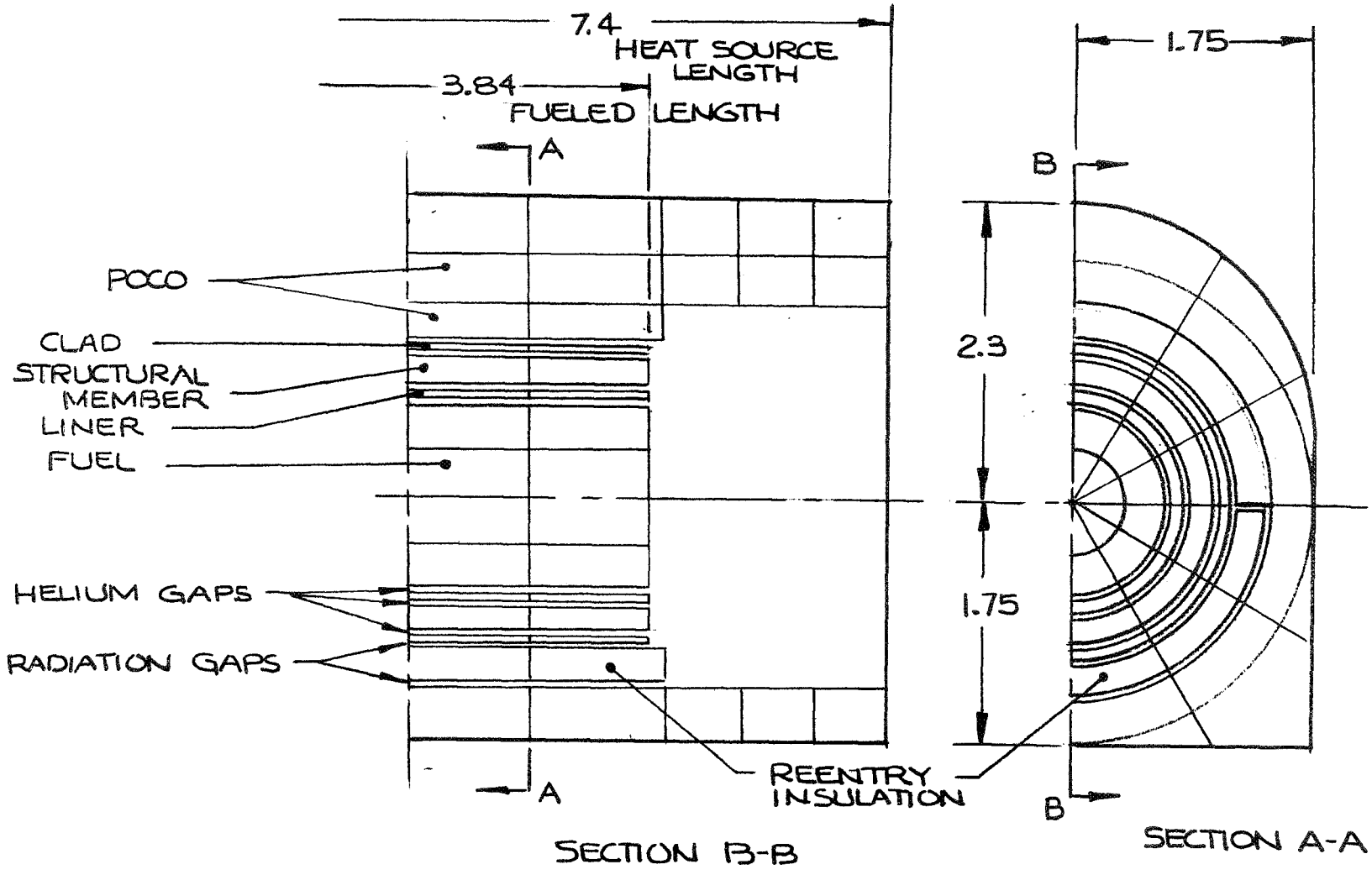

FIGURE 5b THREE DIMENSIONAL THERMAL MODEL OF AN ISOLOAF HEAT SOURCE

FIGURE 6

HEAT SOURCE SURFACE TEMPERATURE VS EMISSIVITY OF HS AND HSHX

PLANAR ARRAY HSU

$T_{HX} = 1670°F$

1BHS FUEL LOAD $Q_{HS} = 400\,w$

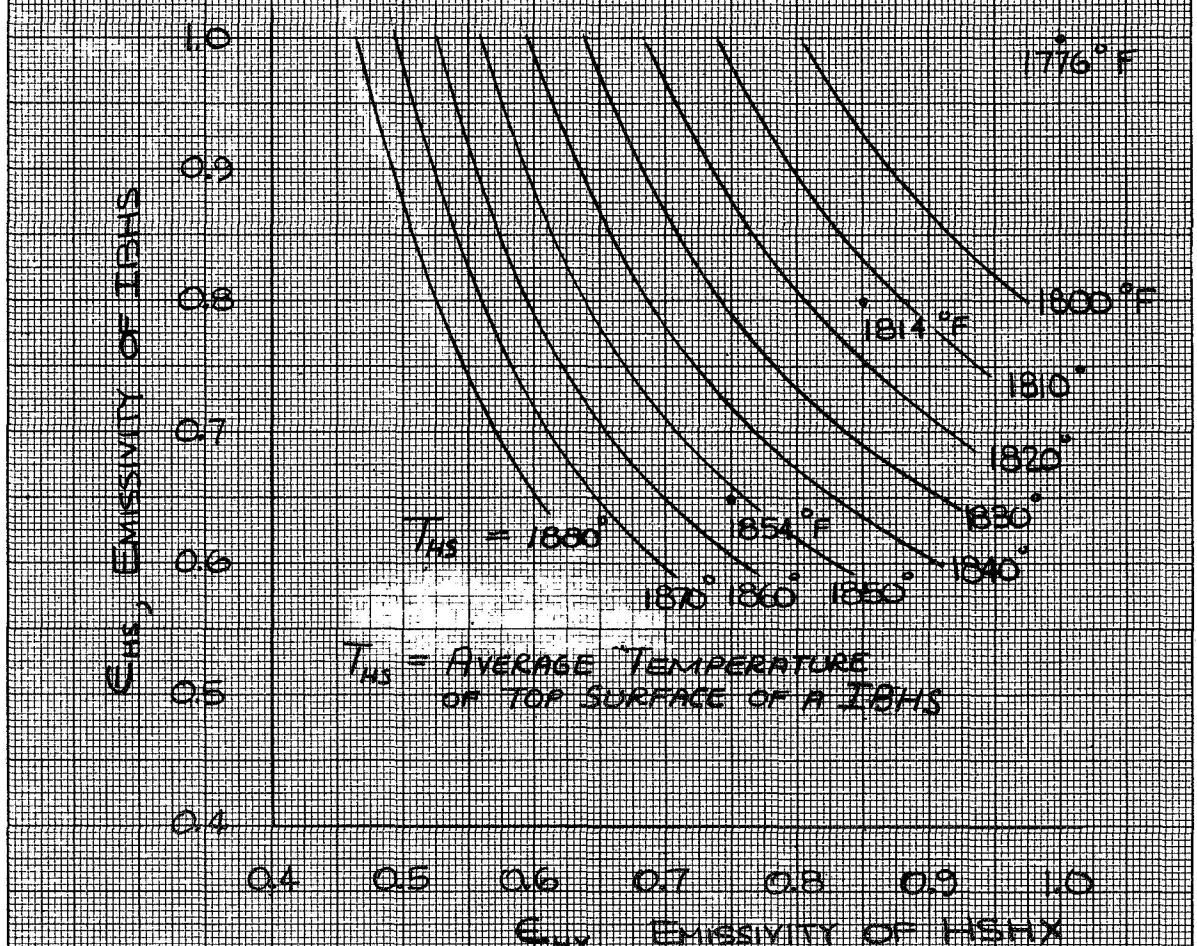

T_{HS} = AVERAGE TEMPERATURE OF TOP SURFACE OF A 1BHS

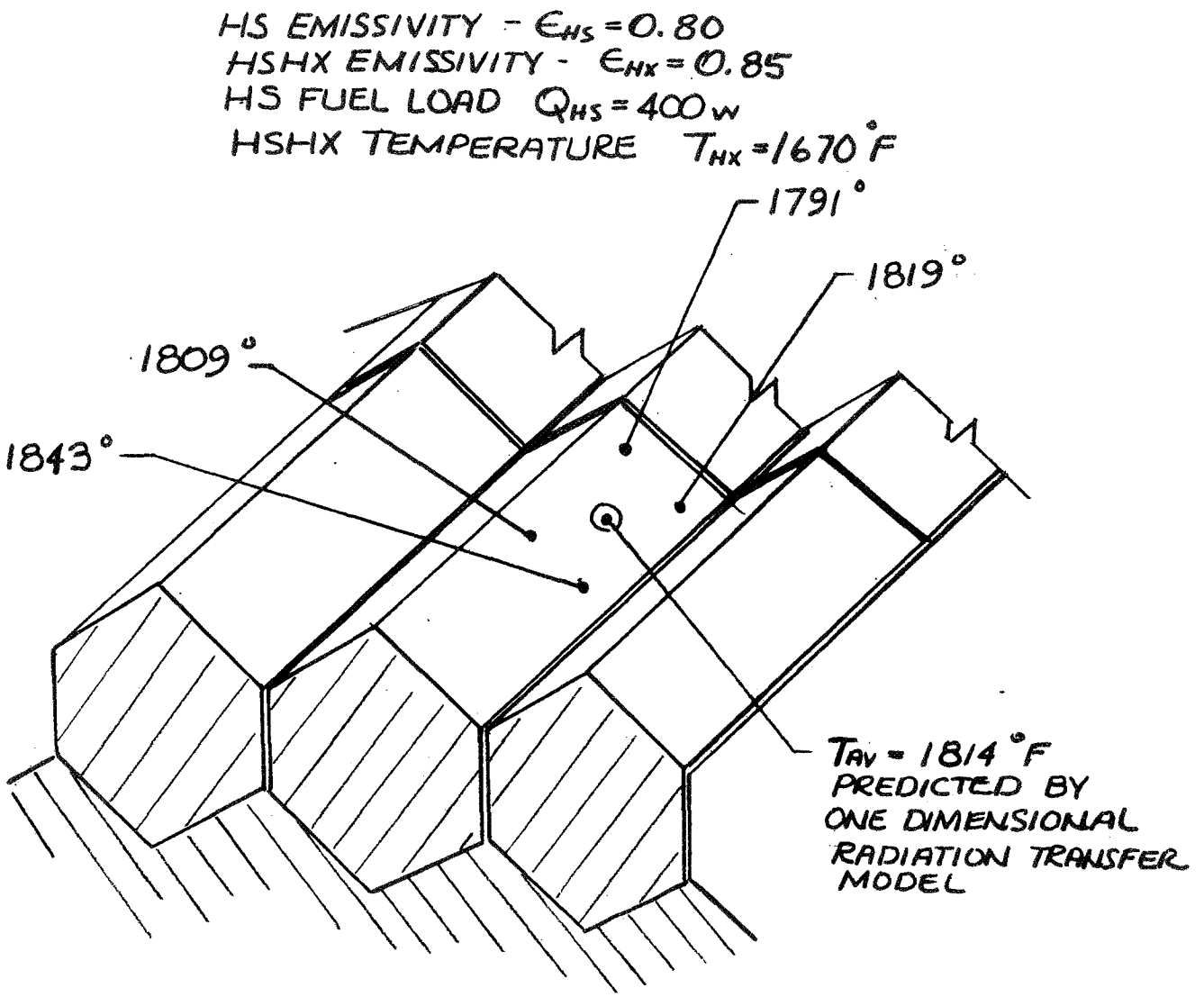

FIGURE 7 HS SURFACE TEMPERATURE FROM 3-D IBHS ANALYSIS

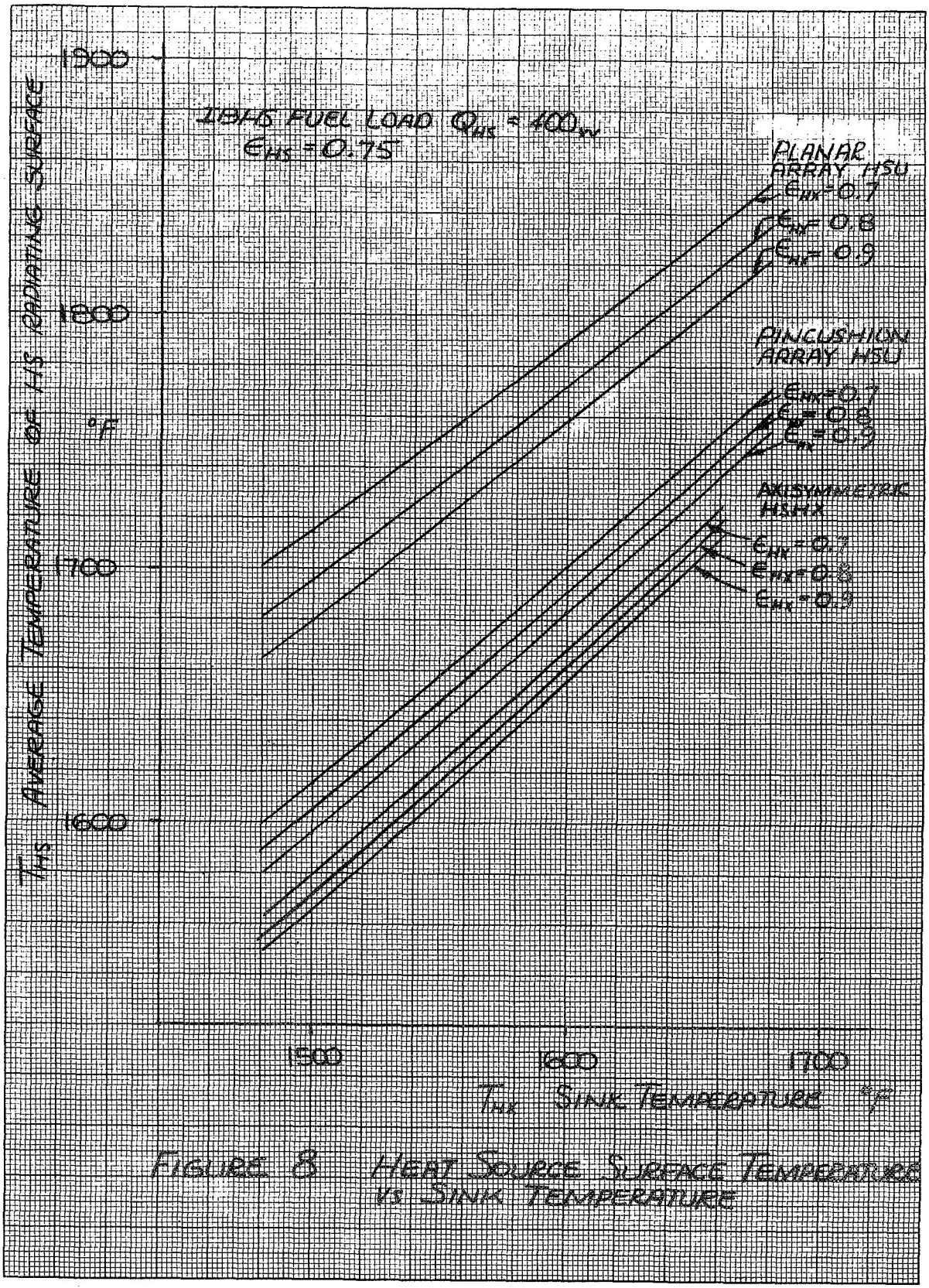

FIGURE 8 HEAT SOURCE SURFACE TEMPERATURE VS SINK TEMPERATURE

FIGURE 9 HEAT SOURCE SURFACE TEMPERATURE VS SINK TEMPERATURE

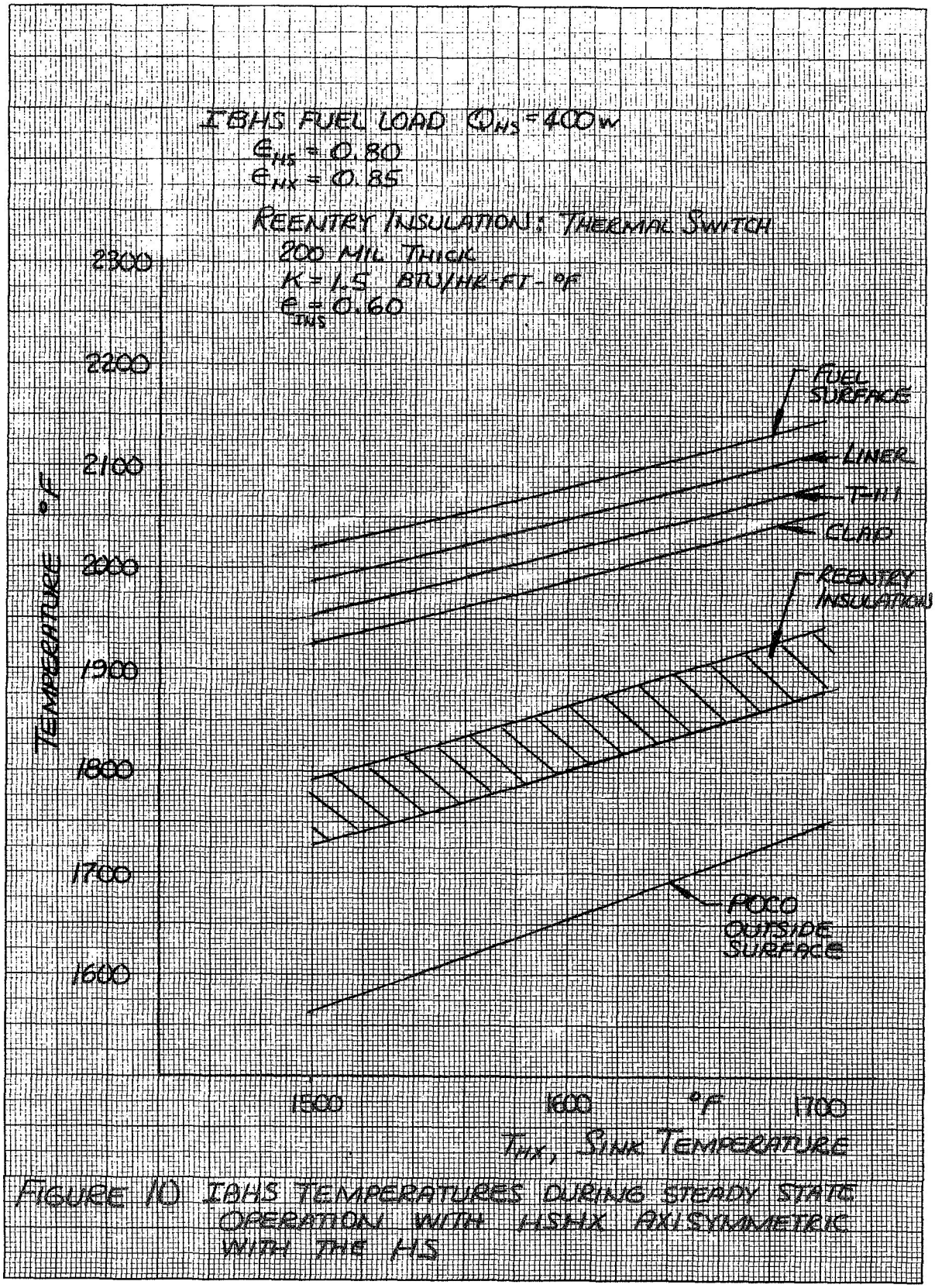

FIGURE 10 IBHS TEMPERATURES DURING STEADY STATE OPERATION WITH HSHX AXISYMMETRIC WITH THE HS

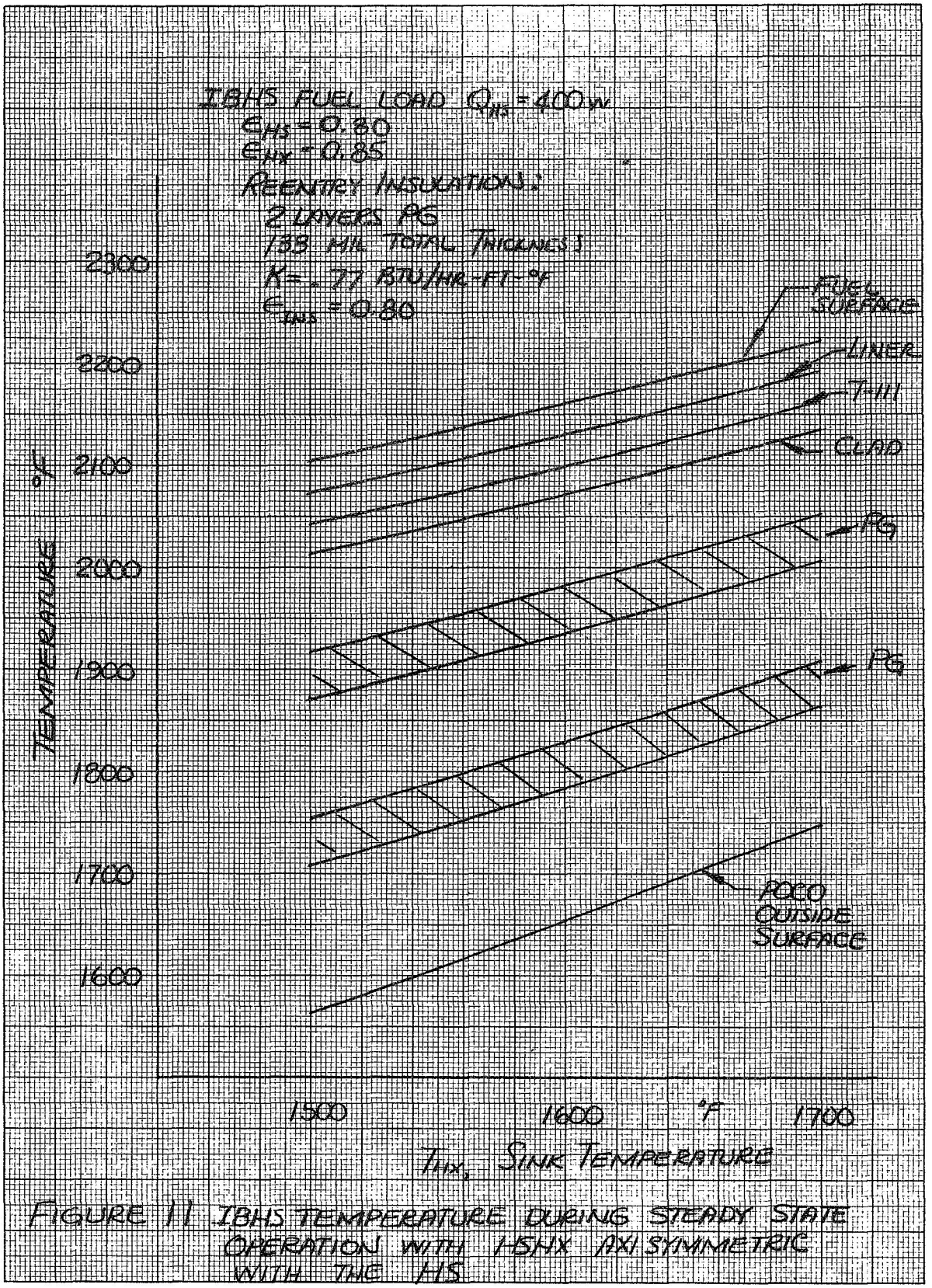

FIGURE 11 IBHS TEMPERATURE DURING STEADY STATE OPERATION WITH 1-SHX AXI SYMMETRIC WITH THE IHS

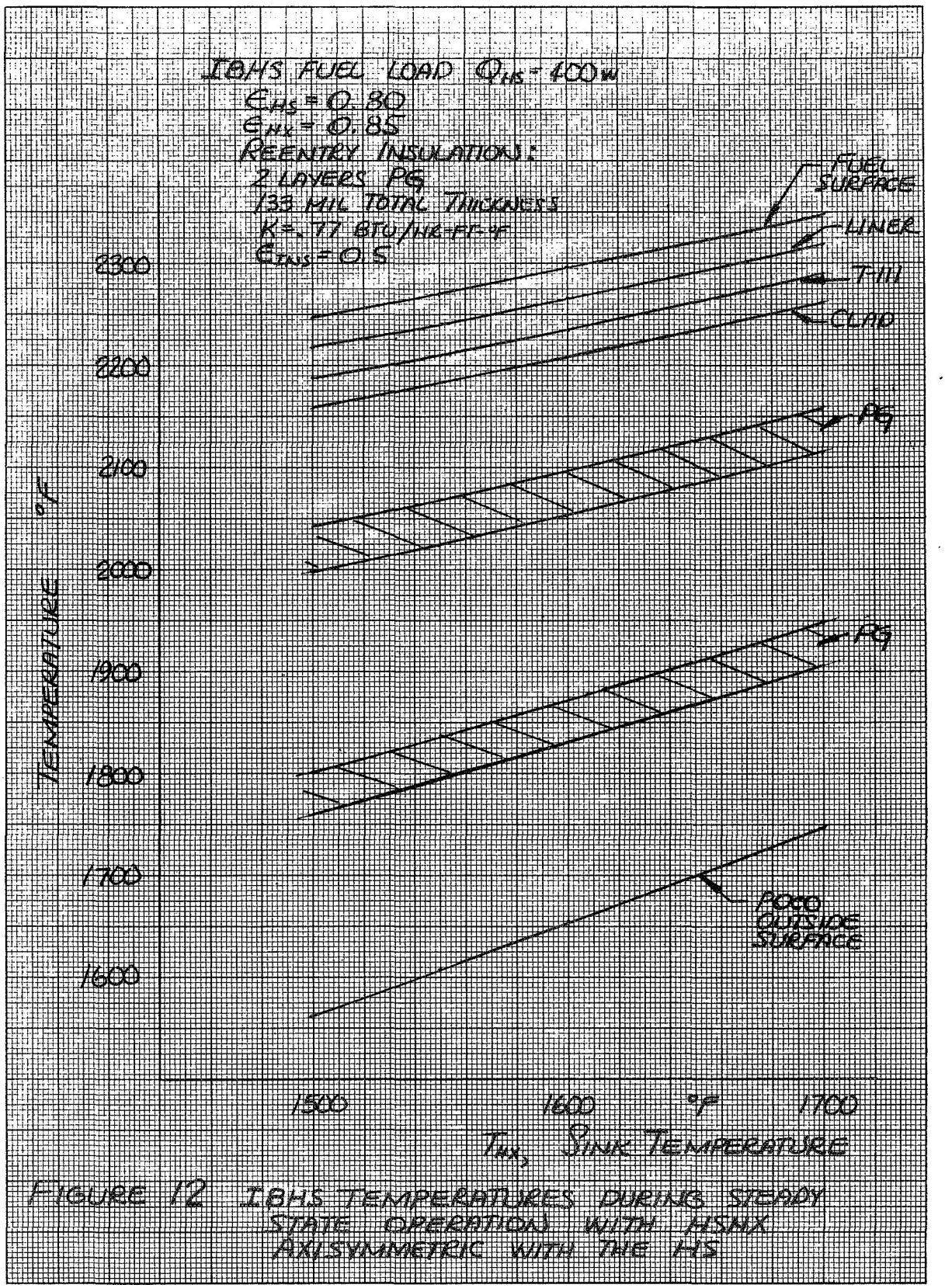

FIGURE 12 IBHS TEMPERATURES DURING STEADY STATE OPERATION WITH HSHX AXISYMMETRIC WITH THE IHS

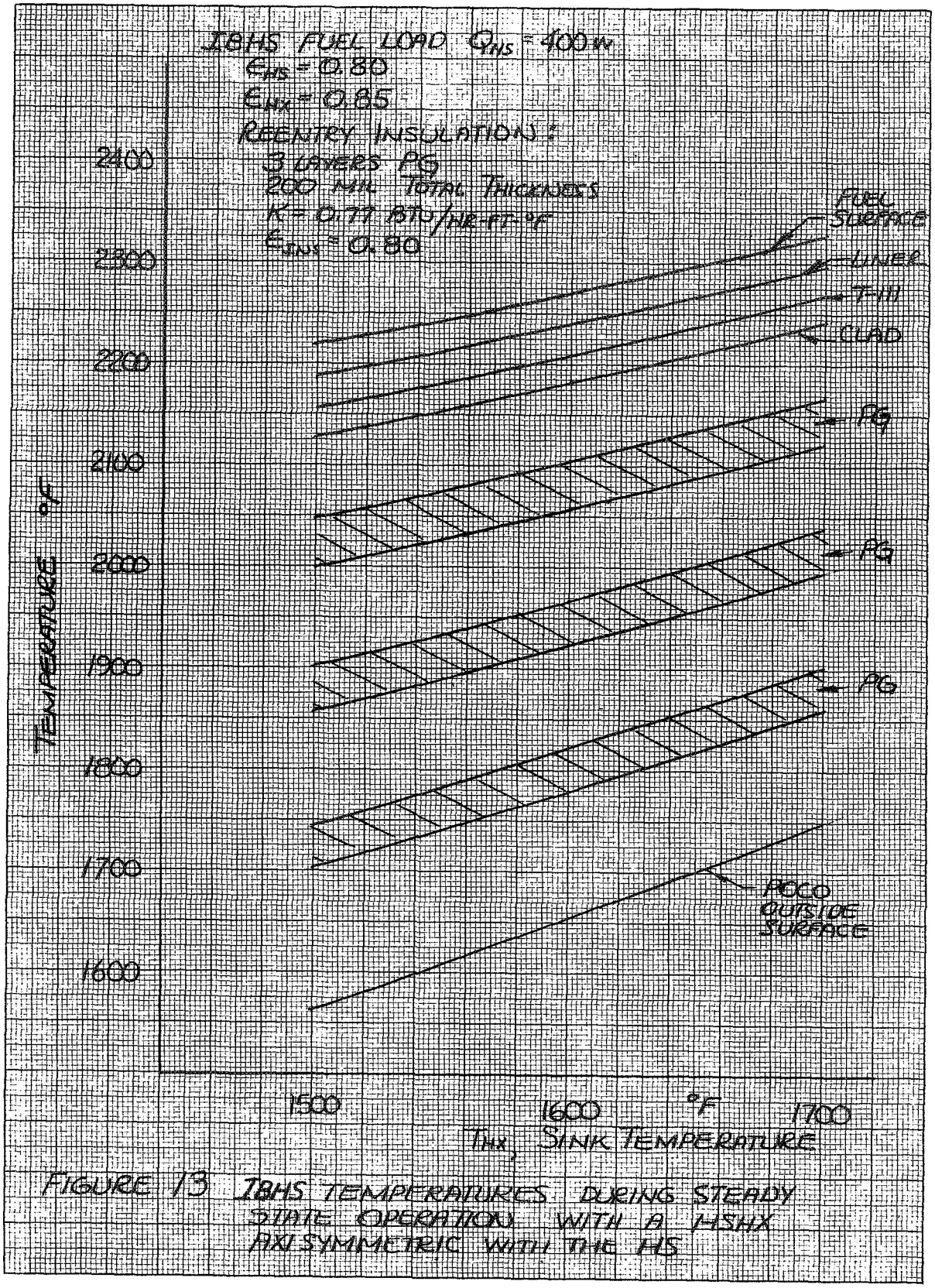

FIGURE 13 IBHS TEMPERATURES DURING STEADY STATE OPERATION WITH A IHSHX AXI SYMMETRIC WITH THE IHS

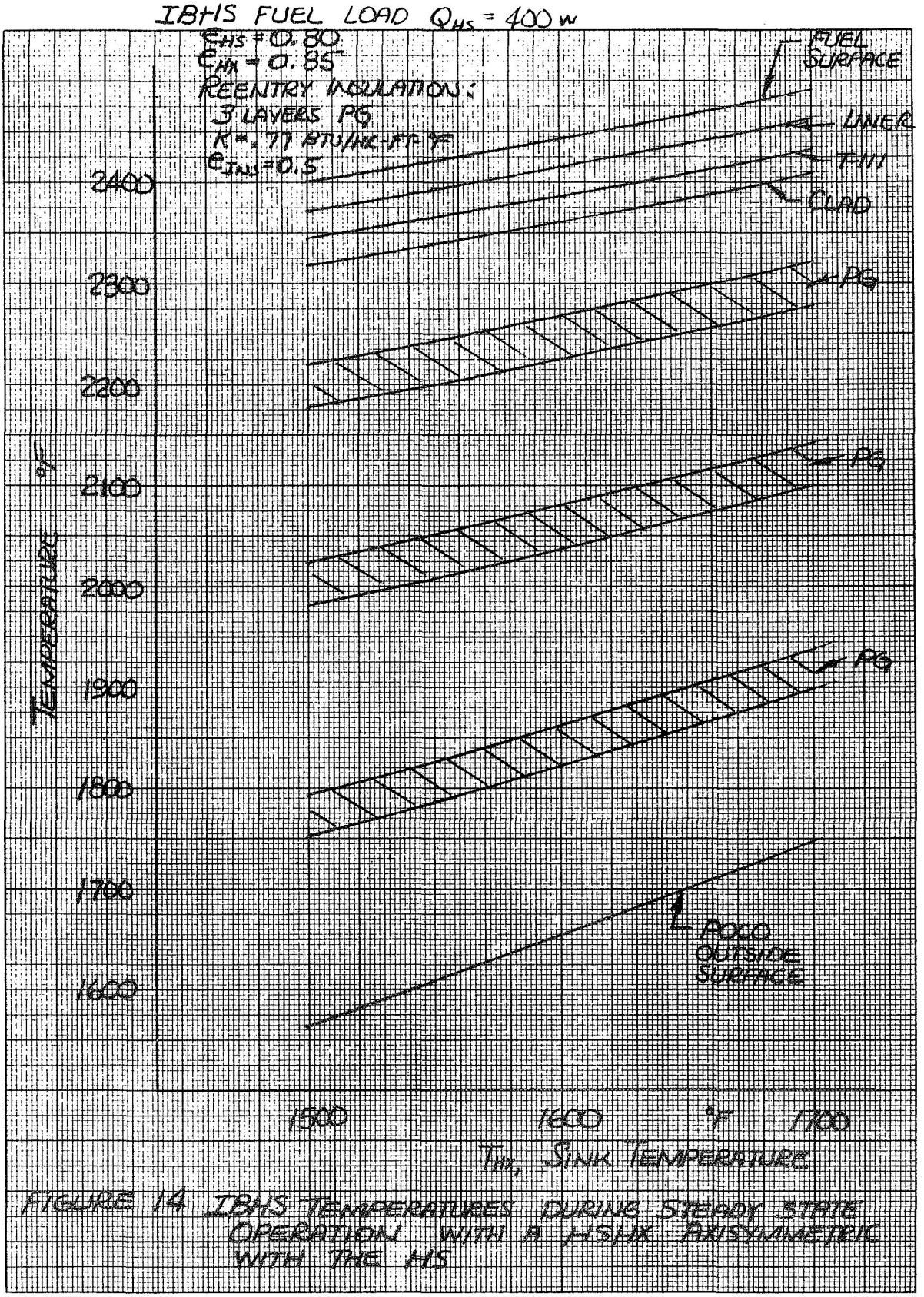

FIGURE 14 IBHS TEMPERATURES DURING STEADY STATE OPERATION WITH A HISHX AXISYMMETRIC WITH THE HS

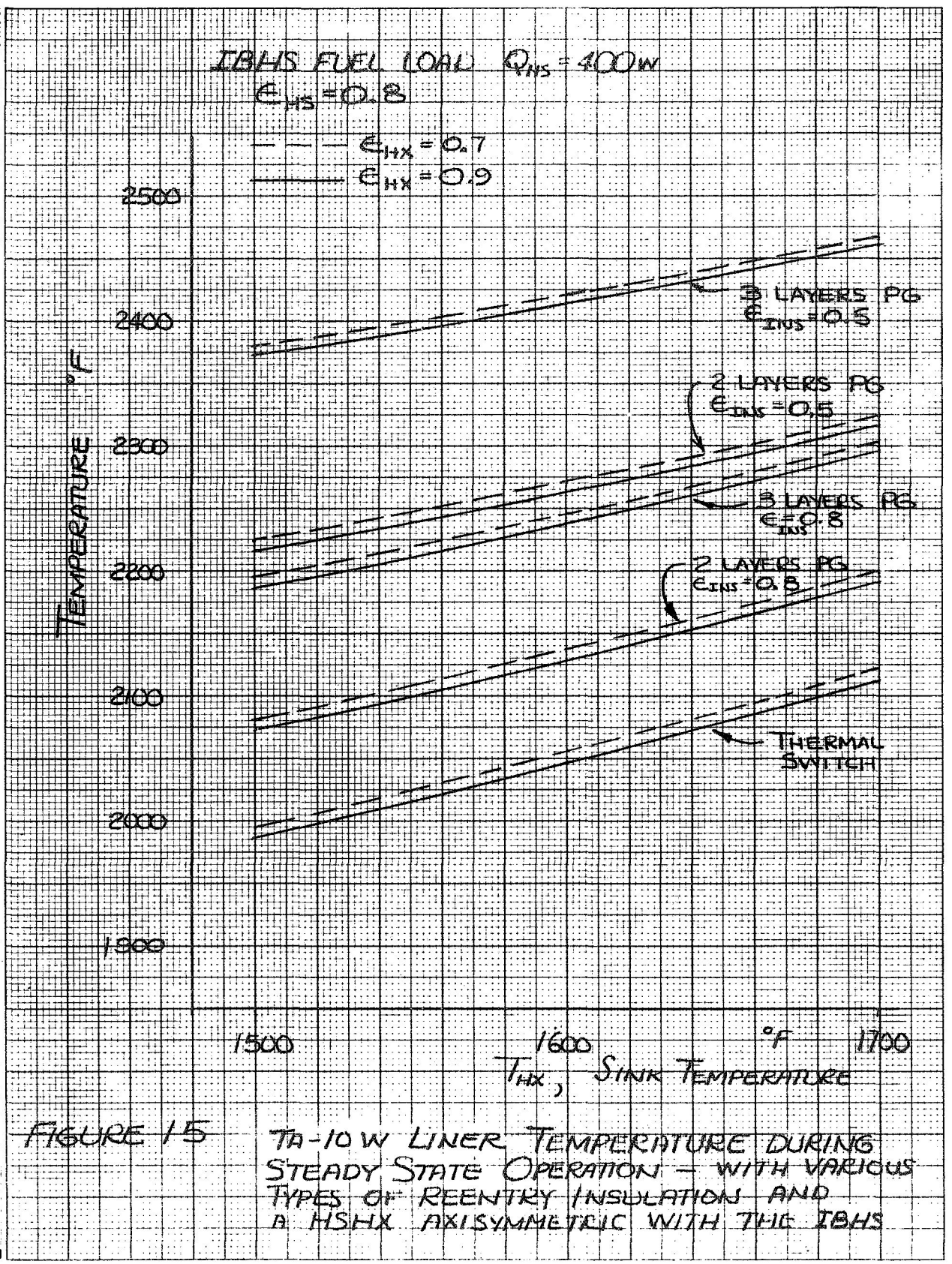

FIGURE 15

TA-10W LINER TEMPERATURE DURING STEADY STATE OPERATION — WITH VARIOUS TYPES OF REENTRY INSULATION AND A HSHX AXISYMMETRIC WITH THE IBHS

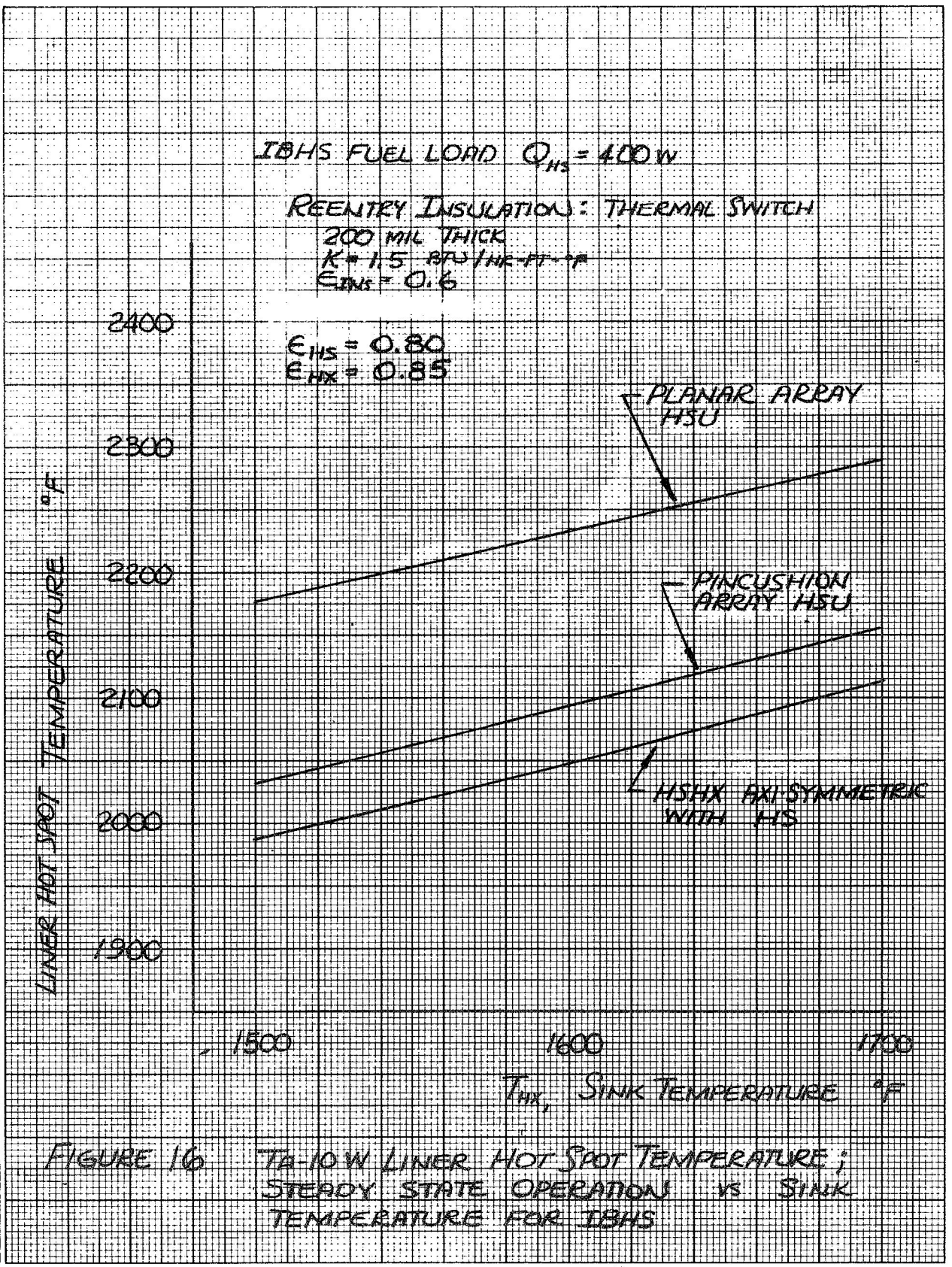

FIGURE 16 TA-10 W LINER HOT SPOT TEMPERATURE; STEADY STATE OPERATION VS SINK TEMPERATURE FOR IBHS

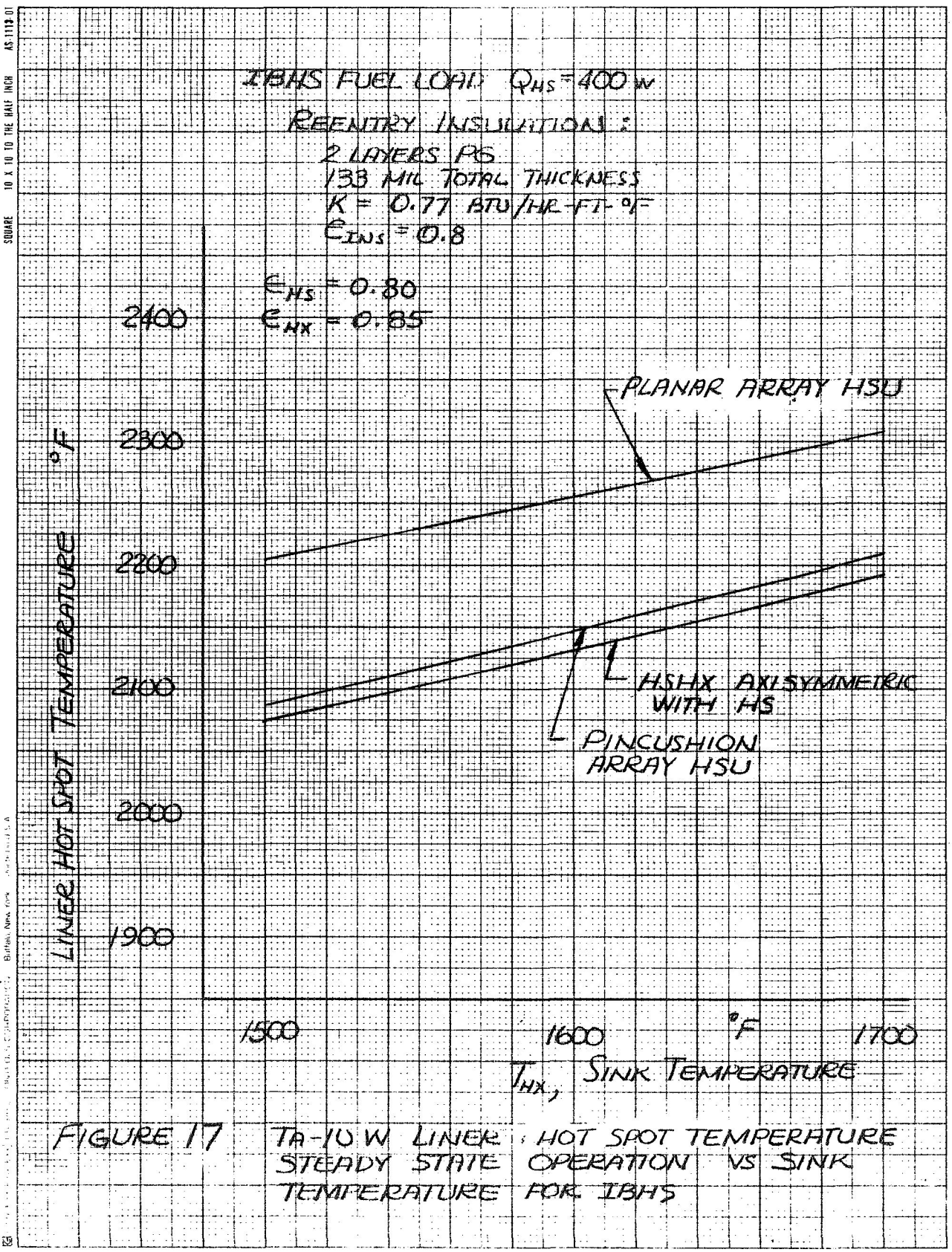

FIGURE 17 TA-10 W LINER HOT SPOT TEMPERATURE STEADY STATE OPERATION VS SINK TEMPERATURE FOR IBHS

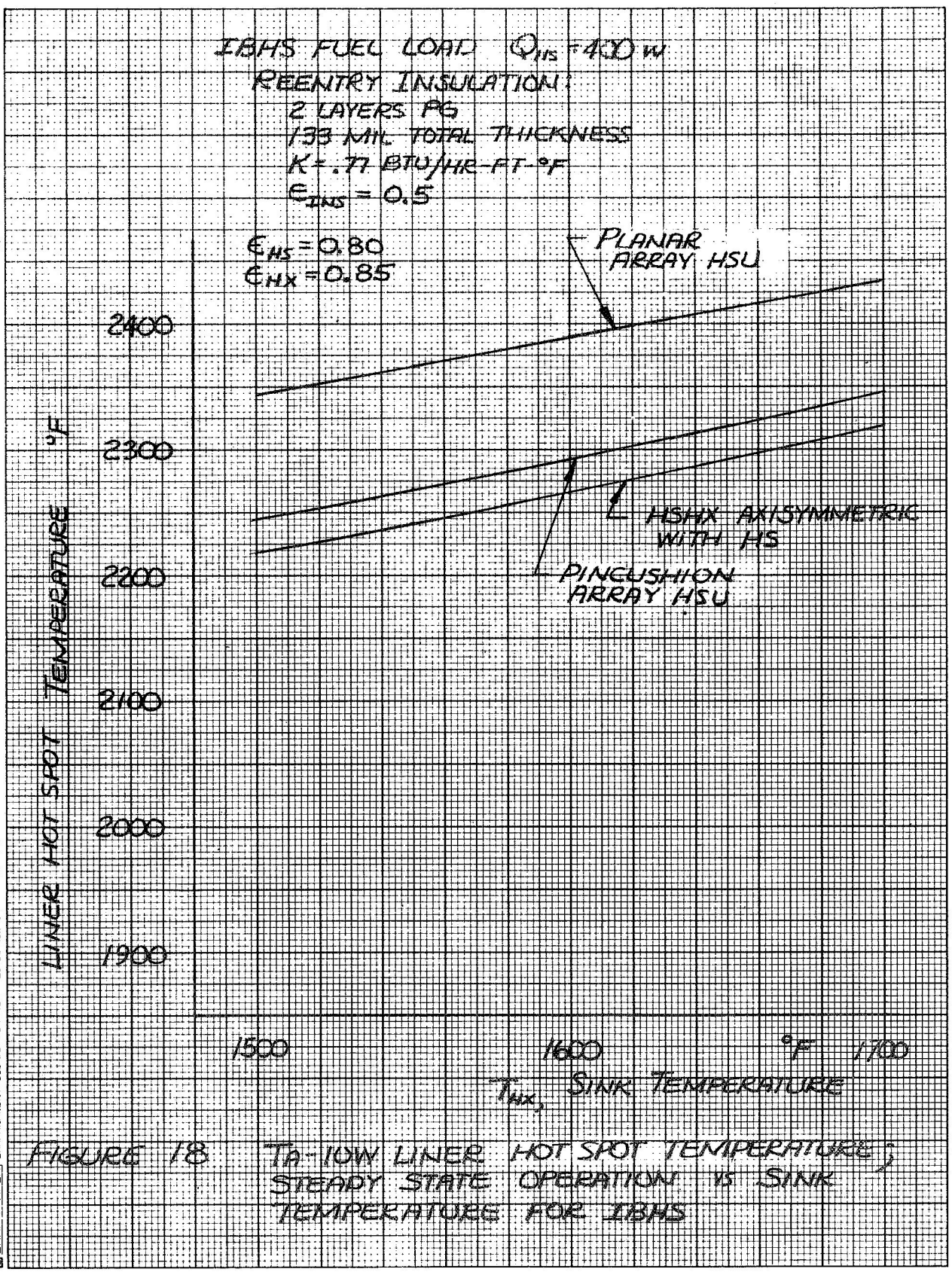

FIGURE 18 T_A - 10W LINER HOT SPOT TEMPERATURE; STEADY STATE OPERATION VS SINK TEMPERATURE FOR IBHS

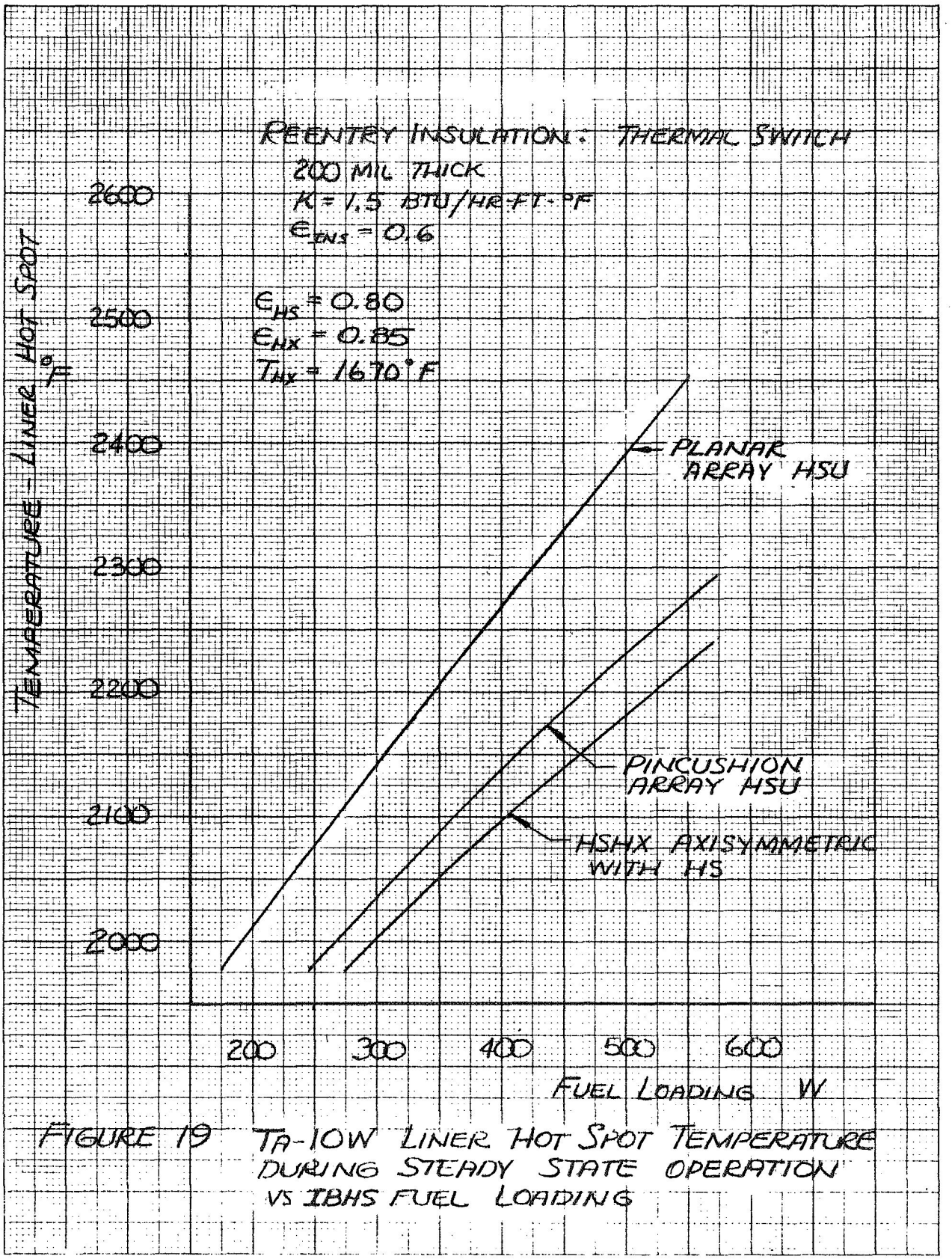

FIGURE 19 TA-10W LINER HOT SPOT TEMPERATURE DURING STEADY STATE OPERATION VS IBHS FUEL LOADING

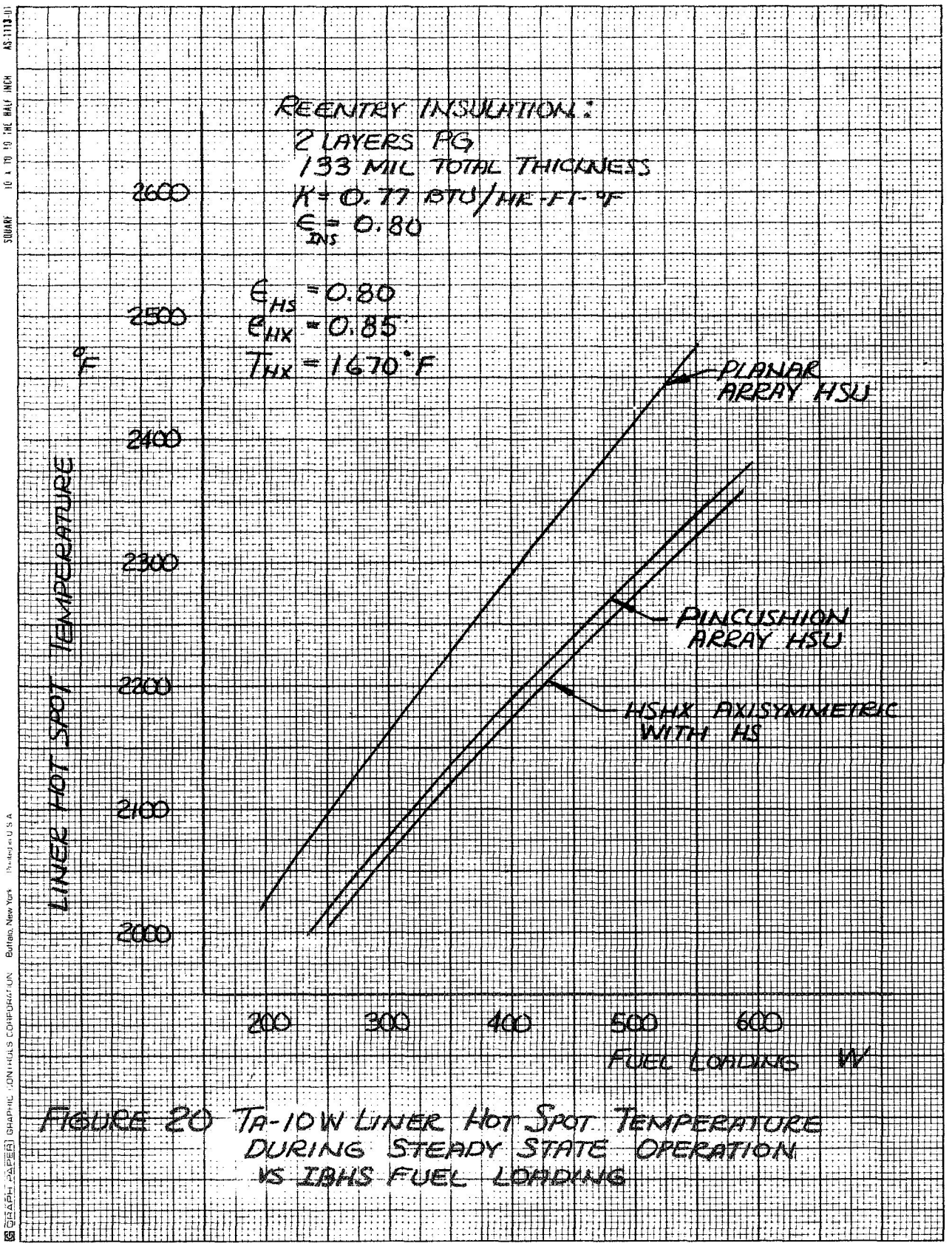

FIGURE 20 TA-10W LINER HOT SPOT TEMPERATURE DURING STEADY STATE OPERATION VS IBHS FUEL LOADING

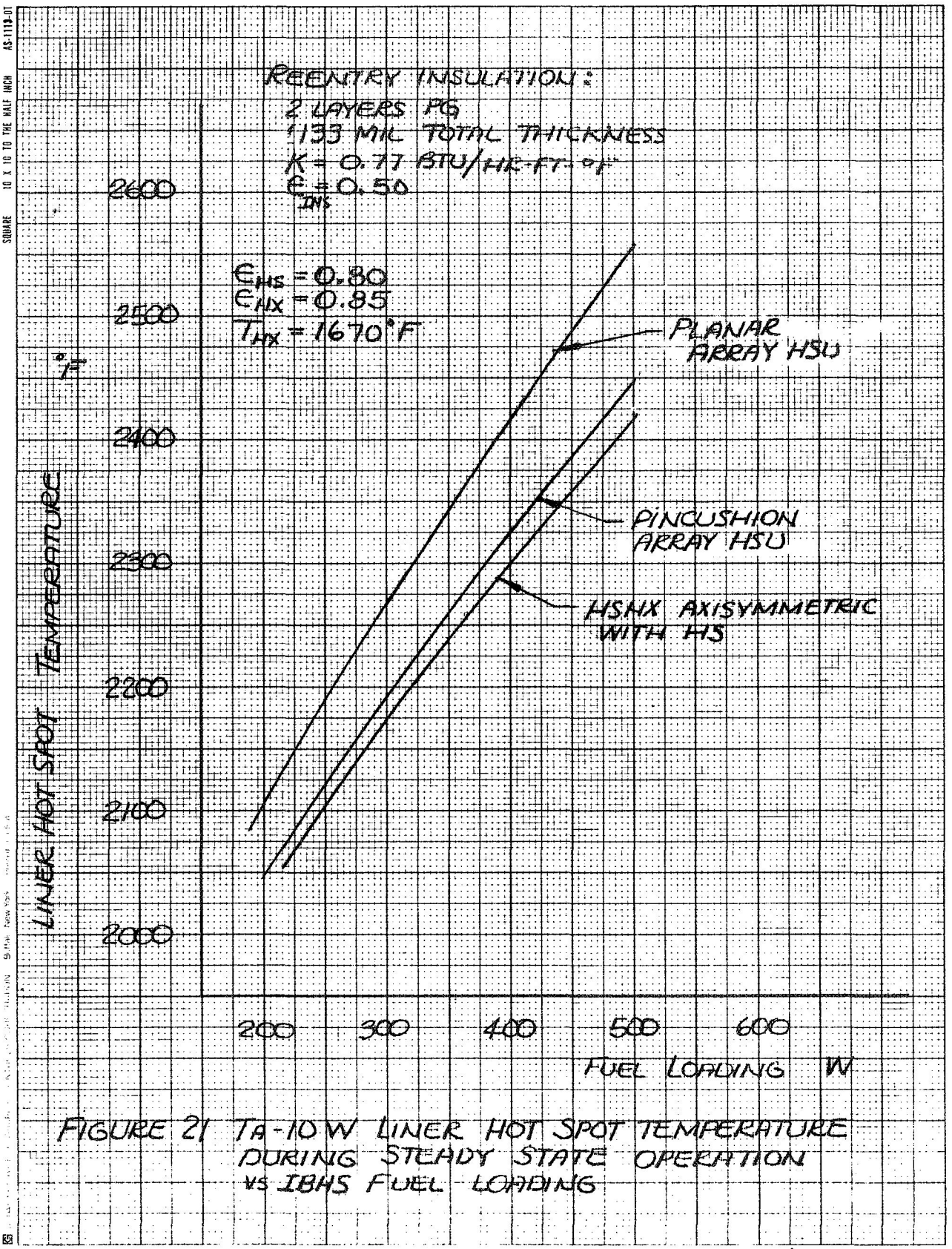

FIGURE 21 T_A-10 W LINER HOT SPOT TEMPERATURE DURING STEADY STATE OPERATION VS IBHS FUEL LOADING

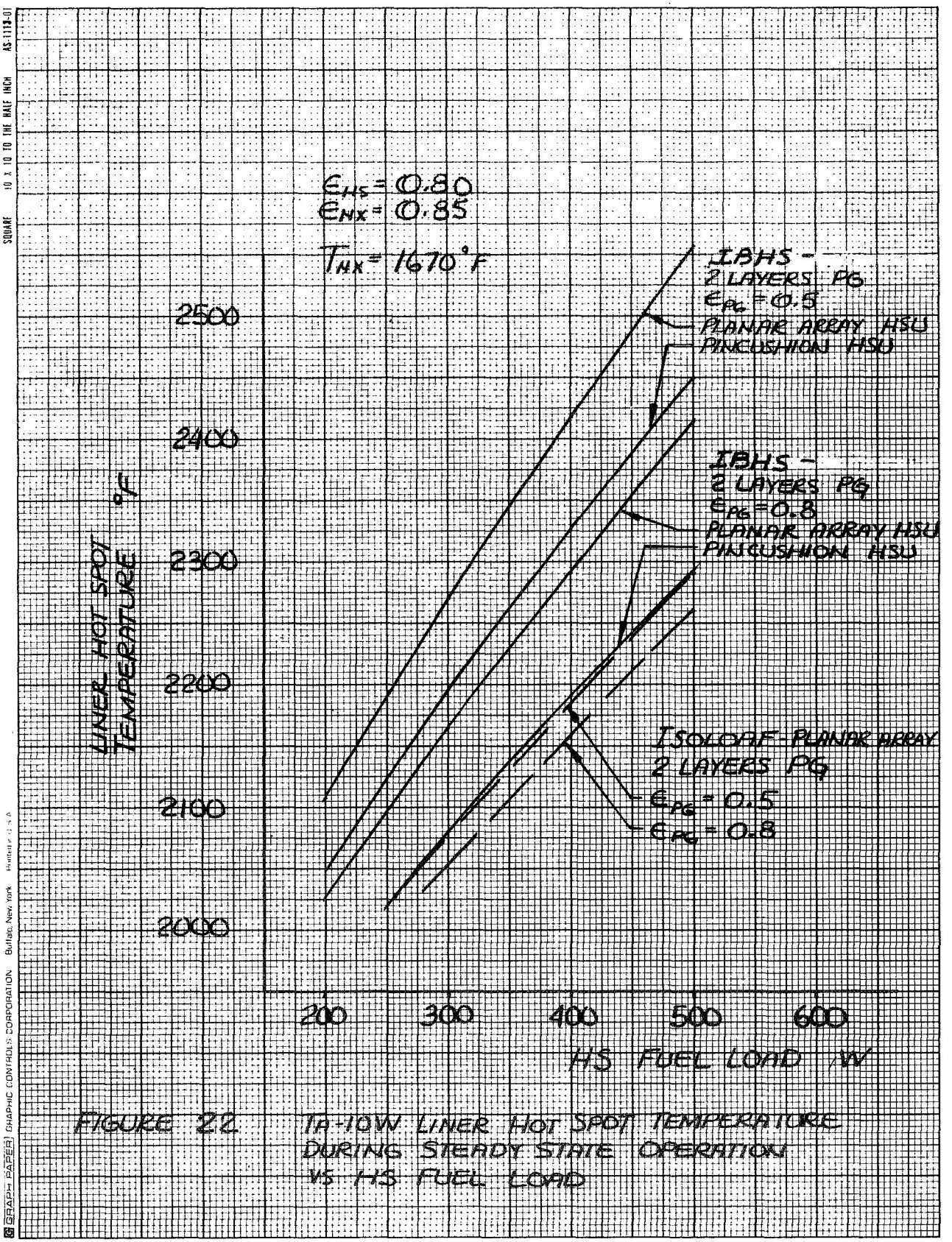

FIGURE 22 TA-10W LINER HOT SPOT TEMPERATURE DURING STEADY STATE OPERATION VS HS FUEL LOAD